



# RESEARCH MEMORANDUM

A THEORETICAL INVESTIGATION OF THE INFLUENCE OF AUXILIARY  
DAMPING IN PITCH ON THE DYNAMIC CHARACTERISTICS OF A  
PROPORTIONALLY CONTROLLED SUPERSONIC  
CANARD MISSILE CONFIGURATION

By Walter C. Nelson and Anthony L. Passera

Langley Aeronautical Laboratory  
Langley Air Force Base, Va.

NATIONAL ADVISORY COMMITTEE  
FOR AERONAUTICS

WASHINGTON

August 25, 1950

NATIONAL ADVISORY COMMITTEE FOR AERONAUTICS

---

RESEARCH MEMORANDUM

---

A THEORETICAL INVESTIGATION OF THE INFLUENCE OF AUXILIARY  
DAMPING IN PITCH ON THE DYNAMIC CHARACTERISTICS OF A  
PROPORTIONALLY CONTROLLED SUPERSONIC  
CANARD MISSILE CONFIGURATION

By Walter C. Nelson and Anthony L. Passera

SUMMARY

A theoretical analysis has been made of a supersonic canard missile configuration to show the means which might be used to improve its dynamic performance characteristics. The analysis was conducted by using the best available estimates of aerodynamic and airframe parameters. The response characteristics were considered with respect to transient-response curves and Nyquist diagrams which were obtained by application of operational calculus and servomechanism theory. The results of the analysis were used to show the means and conditions under which satisfactory performance of the missile could be obtained. Satisfactory system performance was obtained throughout the Mach number and altitude range considered when auxiliary damping was included in the system. Damping was introduced through the canard fins or wing-tip elevators by producing a control deflection proportional to the rate of pitch of the airframe. The rate factor used and the method of adjusting the gain of the autopilot permitted satisfactory performance to be obtained. The procedure used to obtain frequency-response and transient-response characteristics is simple and direct. Nyquist diagrams were useful for system-stability analysis. The manner in which the small static margin and rate control change the shape of the Nyquist diagram to produce good system performance is shown. Pole plots or plots of the roots of the characteristic equation were useful for examining the response characteristics throughout the variation of conditions considered. The plots also indicated the presence of an additional oscillatory mode of motion due to the rate gyro control system.

## INTRODUCTION

As part of the general research program of automatic stabilization, the Pilotless Aircraft Research Division of the Langley Aeronautical Laboratory has been conducting an investigation of the dynamic performance characteristics of an automatically controlled supersonic canard missile configuration. A theoretical analysis of the canard missile configuration discussed herein revealed that its dynamic performance was unsatisfactory when considered with respect to its possible application. The object of the investigation was to show the means which might be used to improve the performance characteristics of a missile for possible guidance applications such as seeker or beam rider systems. The performance qualities of the missile are determined from consideration of the longitudinal frequency-response and transient-response characteristics of the system as calculated from the differential equations of motion assuming two degrees of freedom. The unsatisfactory performance qualities are attributed largely to a lack of inherent aerodynamic damping. Therefore, the damping is increased through a proposed control system which consists of a rate gyroscope-servo combination. This device acts through wing-tip elevators or canard fins to produce a control deflection which is proportional to the rate of pitch of the missile.

The analysis shows how the damping of the system changes with Mach number, altitude, and center-of-gravity location or static margin. Curves are presented to show the circumstances under which the system performance is considered satisfactory and unsatisfactory. Some indication of how much improvement in pitch the system can tolerate as a consequence of acceleration limitations is also given.

## DEFINITIONS AND SYMBOLS

Frequency response.- The frequency response of a linear system is a frequency-dependent function which consists of a phase response and an amplitude response, and expresses the relation between a steady-state sinusoidal input to the system and the steady-state sinusoidal output of the system. The phase response gives the time displacement between the input and output expressed as an angle and the amplitude response gives the ratio of the peak amplitudes of the input and output.

Closed-loop response.- The closed-loop response is the frequency or transient response of a system where the output is used as a feedback to modify the input.

Open-loop response.- The open-loop response is the frequency or transient response of a system when the outer feedback loop is open. (See block diagram on page 6.)

Nyquist diagram.- A Nyquist diagram is a polar plot of the open-loop frequency response.

Static margin.- The distance between the center of gravity and the center of pressure in mean aerodynamic chords,  $\frac{C_{m\alpha}}{C_{L\alpha}}$ .

Y	stability axis which passes through the center of gravity and is perpendicular to the plane of the vertical wings
I <sub>y</sub>	moment of inertia about the Y-axis, 30 slug feet square
m	mass, 4.66 slugs
c	wing chord, 1.395 feet
S	exposed wing area, 2.52 square feet
q	dynamic pressure, pounds per square foot
q	$\frac{\dot{\theta}c}{2V}$ (when used as a subscript)
V	velocity, feet per second
$\zeta$	damping ratio
$\omega$	frequency, radians per second
$\omega_n$	natural frequency, radians per second
K <sub>r</sub>	gyroscope rate factor
K <sub>A</sub>	autopilot gain factor, a constant
$\delta_r$	canard-fin or wing-tip control-surface-deflection angle due to rate of pitch, radians
$\delta_s$	canard-fin-deflection angle produced by autopilot, radians
$\delta_t$	wing-tip control-surface-deflection angle, radians
$\theta$	pitch angle measured from horizontal, radians
$\alpha$	angle of attack, radians
t	time, seconds

$\gamma$	flight-path angle measured from horizontal, radians
$g$	acceleration due to gravity
$j$	$\sqrt{-1}$
$p$	Laplace transform variable corresponding to the differential operator $D \equiv \frac{d}{dt}$
$u$	nondimensionalized frequency variable $\frac{\omega}{\omega_n}$
$\dot{\theta}, \ddot{\theta}, \dot{\alpha}, \ddot{\alpha}$	denote derivatives with respect to time, that is, $\frac{d\theta}{dt}$ , $\frac{d^2\theta}{dt^2}$ , $\frac{d\alpha}{dt}$ , and $\frac{d^2\alpha}{dt^2}$ , respectively
$M$	Mach number
$C_L$	lift coefficient
$C_m$	moment coefficient
$C_{L\alpha}$	$\frac{\partial C_L}{\partial \alpha}$
$C_{m\alpha}$	$\frac{\partial C_m}{\partial \alpha}$
$C_{mq}$	$\frac{\partial C_m}{\partial \frac{\dot{\theta} c}{2V}}$
$C_{m\dot{\alpha}}$	$\frac{\partial C_m}{\partial \frac{\dot{\alpha} c}{2V}}$
$C_{L\delta_s}$	$\frac{\partial C_L}{\partial \delta_s}$
$C_{m\delta_s}$	$\frac{\partial C_m}{\partial \delta_s}$

$$C_{L\delta_t} \quad \frac{\partial C_L}{\partial \delta_t}$$

$$C_{m\delta_t} \quad \frac{\partial C_m}{\partial \delta_t}$$

$$C_{L\delta_r} \quad \frac{\partial C_L}{\partial \delta_r}$$

$$C_{m\delta_r} \quad \frac{\partial C_m}{\partial \delta_r}$$

Subscripts:

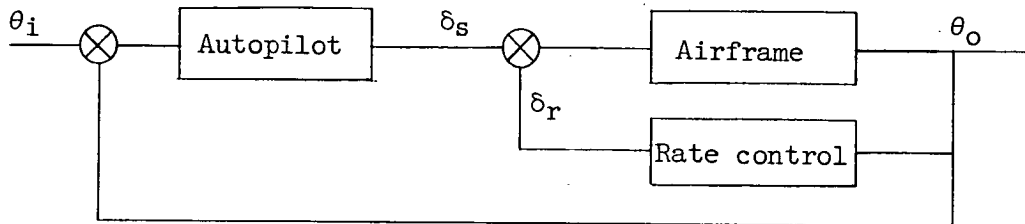
- i        input or forcing function, corresponding to a command calling for a change in heading or to a sinusoidal input variation
- o        output or response function, for example, the system response to a command signal or to a sinusoidal input variation

#### DESCRIPTION OF MISSILE CONFIGURATION AND RATE-CONTROL SYSTEM

The missile used in this report is a symmetrical cruciform configuration as shown in figure 1. A flight test of this configuration is reported in reference 1. The wings and canard fins are of delta design with the leading edges swept back  $60^\circ$ . The wing airfoil section is a modified double wedge and the fuselage fineness ratio is 16:1. The horizontal canard fins and wing tips have the same plan form, the wing tips having a double-wedge cross section while the canard fins have beveled leading and trailing edges. The canard fins, however, provide the required longitudinal control while the auxiliary damping is provided either through the canard fins or the wing-tip elevators. To obtain the additional damping, a rate gyro-servo combination is proposed. The rate gyro-servo system was considered to be a single-degree-of-freedom system with a natural frequency of 88 radians per second and 0.5 critically damped. The control then has a reasonably flat response up to and beyond the highest natural frequency anticipated from the missile. The estimated aerodynamic derivatives and parameters of the configuration as used in the calculations are given in tables I, II, and III.

## ANALYSIS

The purpose of this paper is to show the conditions under which it is possible to obtain satisfactory longitudinal performance from the supersonic missile configuration discussed herein. The following block diagram can be used to represent the system in its most general form and can be regarded as a double-loop servomechanism:



The input  $\theta_i$  is a signal, possibly from a seeker, which calls for a change in attitude of the missile. The frequency response of the autopilot is assumed to be a constant with zero phase change at all frequencies. This means that any signal entering the autopilot is multiplied by a constant factor  $K_A$  called the autopilot gain and there is no time lag in the output signal. The equation for the autopilot response is

$$\delta_s = K_A(\theta_i - \theta_o)$$

The rate-control system acts on the output of the airframe and produces a control deflection proportional to the rate of pitch. The differential equation for the control motion producing additional damping is

$$\ddot{\delta}_r + 2\zeta\omega_n\dot{\delta}_r + \omega_n^2\delta_r = K_r\dot{\theta} \quad (1)$$

where  $\zeta = 0.5$ ,  $\omega_n = 88$  radians per second, and  $K_r = 518$  when the rate control is assumed to operate on the canard fins.

The equations of motion for the missile with rate control as used in this analysis, assuming two degrees of freedom with constant forward velocity and straight and level flight, are

$$\left. \begin{aligned} \frac{I_y}{qSc} \ddot{\theta} - C_{mq} \frac{c}{2V} \dot{\theta} - C_{m\dot{\alpha}} \frac{c}{2V} \dot{\alpha} - C_{m\alpha} \alpha &= C_{m\delta_s} \delta_s + C_{m\delta_r} \delta_r \\ \frac{mV}{qS} \dot{\theta} - \frac{mV}{qS} \dot{\alpha} - C_{L\alpha} \alpha &= C_{L\delta_s} \delta_s + C_{L\delta_r} \delta_r \end{aligned} \right\} \quad (2)$$

These functions are assumed to be linear differential equations with constant coefficients.

The analysis shows the method used to obtain various frequency-response and transient-response data for the longitudinal missile motions when the proposed rate control is included in the system. A complete treatment of the method outlined here for finding the frequency response can be found on pages 243-250 of reference 2. The most general form of the solutions used in this paper will be outlined. Because the form is general it can be used to find various missile responses when rate control is not included if the terms pertaining to the rate control are called zero.

The transfer function  $\frac{\theta_o}{\delta_s}(p)$  for the missile with auxiliary damping is obtained by taking the Laplace transform of equations (1) and (2) and then substituting equation (1) in (2). It is assumed that at zero time

$$\theta = \dot{\theta} = \ddot{\theta} = \alpha = \dot{\alpha} = 0$$

The method of transforming the differential equations of motion can be found in reference 3. This procedure yields an algebraic function of the form

$$\frac{\theta_o}{\delta_s}(p) = \frac{a_3 p^3 + a_2 p^2 + a_1 p + a_0}{p^5 + b_4 p^4 + b_3 p^3 + b_2 p^2 + b_1 p} \quad (3)$$

where the a's and b's are constants. Equation (3) can be rewritten in the form

$$\frac{\theta_o}{\delta_s}(p) = K_p \frac{(p + \sigma)(p^2 + 2\zeta_1 \omega_{n1} p + \omega_{n1}^2)}{p(p^2 + 2\zeta_2 \omega_{n2} p + \omega_{n2}^2)(p^2 + 2\zeta_3 \omega_{n3} p + \omega_{n3}^2)} \quad (4)$$

where  $K_p$ ,  $\sigma$ , and the  $\zeta$ 's and  $\omega_n$ 's are constants. Following the

usual procedure of putting  $p = j\omega$ , (4) is nondimensionalized by the change of variable

$$u = \frac{\omega}{\omega_{n1}}$$

Equation (4) then becomes

$$\frac{\theta_o}{\delta_s}(ju) = K_u \frac{(\tau_1 ju + 1)(-u^2 + 2\xi_1 ju + 1)}{ju(-\tau_2^2 u^2 + 2\tau_2 \xi_2 ju + 1)(-\tau_3^2 u^2 + 2\tau_3 \xi_3 ju + 1)} \quad (5)$$

where  $K_u$ , the  $\tau$ 's, and  $\xi$ 's are constants. With such an algebraic function there are only four possible types of terms which can occur, the forms of which are

- (a) a constant ( $K_u$ )
- (b)  $ju$
- (c)  $(\tau ju + 1)$
- (d)  $(-\tau^2 u^2 + 2\xi \tau ju + 1)$

If the logarithm of equation (5) is taken, the right side of the resulting equation is the sum of the logarithm of factors of the types listed. This logarithmic form permits the use of a series of templates for plotting the amplitude and phase versus nondimensional frequency  $u$  for each component of  $\frac{\theta_o}{\delta_s}(ju)$ . A summation of the amplitude components and the phase components results in a logarithmic plot of the frequency response. Conventional servomechanism theory usage of expressing the amplitude ratio in decibels is employed herein as follows:

$$\text{The magnitude of } \frac{\theta_o}{\delta_s}(ju) \text{ in decibels} = 20 \log_{10} \frac{\theta_o}{\delta_s}(ju)$$

Nyquist diagrams are used in this report to study the frequency-response characteristics of the missile. For example, a Nyquist diagram of the open-loop frequency response reveals whether or not the closed-loop system is stable. This can be discerned by observing if the critical point  $(-1,0)$  is enclosed. A rigorous mathematical interpretation of this stability criterion can be found in reference 4. The frequency response of a system is useful because preliminary estimates can be made from it concerning the transient-response qualities of the system.

To obtain Nyquist diagrams for the missile system, points were read directly off the phase and amplitude plots of the frequency response which was obtained by graphical composition of the  $\frac{\theta_o}{\delta_s}(ju)$  components, as previously explained. The points for the amplitude response were reconverted from decibels and the results were plotted in polar form.

The response qualities of the missile system of this paper are determined from a study of the open-loop frequency response and the closed-loop transient response. The method of obtaining the open-loop frequency response has been demonstrated. The following procedure was used to find the closed-loop transient response. According to reference 2 page 86, equation (3) can be used to find the closed-loop transfer function by applying the formula

$$\frac{\theta_o(p)}{\theta_i} = \frac{K_A \frac{\theta_o(p)}{\delta_s}}{1 + K_A \frac{\theta_o(p)}{\delta_s}} \quad (6)$$

A method for changing the autopilot gain to improve the closed-loop transient response will be demonstrated later.

The transient responses considered in this report are the responses of the missile system to a unit-step input. If  $\theta_i(t)$  is the input, reference 3 shows that the transform of a unit step input can be represented by

$$\theta_i(p) = \frac{1}{p}$$

Substituting this input and equation (3) into equation (6) yields a function of the form

$$\theta_o(p) = \frac{1}{p} \frac{a_3 p^3 + a_2 p^2 + a_1 p + a_0}{b_5 p^5 + b_4 p^4 + b_3 p^3 + b_2 p^2 + b_1 p + b_0} \quad (7)$$

where the  $a$ 's and  $b$ 's are constants. Equation (7) can be rewritten in the form

$$\theta_o(p) = \frac{K_1}{p + z_1} + \frac{K_2}{p + z_2} + \frac{K_3}{p + z_3} + \frac{K_4}{p + z_4} + \frac{K_5}{p + z_5} + \frac{K_6}{p + z_6} \quad (8)$$

where the  $K$ 's and  $z$ 's are, in general, complex constants. The transient response  $\theta_o(t)$  is determined from equation (8) by taking

the inverse transform as explained in reference 3. In this investigation the sextic denominator of equation (7) has one root which is zero, one which is real, and four which are complex. These roots are also called poles of  $\theta_o(p)$ . Because of the character of the poles of  $\theta_o(p)$ , the inverse transform of equation (8) yields a response function of the form

$$\theta_o(t) = 1 + C_1 e^{\alpha_1 t} + C_2 e^{\alpha_2 t} \cos \beta_1 t + C_3 e^{\alpha_2 t} \sin \beta_1 t + C_4 e^{\alpha_3 t} \cos \beta_2 t + C_5 e^{\alpha_3 t} \sin \beta_2 t \quad (9)$$

where the C's,  $\alpha$ 's, and  $\beta$ 's are all real constants.

In addition to the transient  $\theta_o(t)$  responses some responses were also found for angle of attack and normal acceleration. This was done for those cases where the greatest accelerations were anticipated as seen from the shapes of the  $\theta_o(t)$  curves. To find the angle of attack and acceleration responses, the differential equations of motion were first solved for  $\frac{\alpha}{\delta_s}(p)$ . This function, supplemented by  $\frac{\theta_o}{\delta_s}(p)$  and  $\frac{\theta_o}{\theta_i}(p)$ , as determined previously, was used to find  $\frac{\alpha}{\theta_i}(p)$  by applying the formula

$$\frac{\alpha}{\theta_i}(p) = \frac{\theta_o}{\theta_i}(p) \cdot \frac{\frac{\alpha}{\delta_s}(p)}{\frac{\theta_o}{\delta_s}(p)} \quad (10)$$

The angle of attack  $\alpha(t)$  is obtained from equation 10 in the same manner that  $\theta_o(t)$  was solved for. Having found  $\alpha(t)$ , the relationship

$$\gamma(t) = \theta_o(t) - \alpha(t)$$

was used to find  $\dot{\gamma}(t)$ . The longitudinal acceleration in g's is then given by

$$g(t) = \frac{V}{57.3g} \dot{\gamma}(t)$$

The transient-response qualities are used to examine and establish performance criteria. The transient response of a system is considered satisfactory when the output closely follows the input. Before the transient-response data  $\theta_o(t)$  could be obtained, it was necessary to find the roots of the equation of  $\theta_o(p)$ . These roots are called poles of  $\theta_o(p)$  and they determine such qualities as frequency and damping in the transient response of a system. A pole with a large imaginary part reveals an oscillatory mode of motion with a high natural frequency, and if the real part is large negative the oscillatory mode will damp out quickly with increasing time after a disturbance has been applied. The position of the poles in the complex plane for various conditions of flight has the convenience of condensing a large amount of information about the system on a single plot.

The method of obtaining the response characteristics of the missile has been demonstrated. To determine the conditions under which satisfactory system performance could be obtained, the missile responses were found when the proposed rate control was included and left out of the system. The estimated aerodynamic data were used to find the open- and closed-loop transfer functions  $\frac{\theta_o}{\delta_s}(p)$  and  $\frac{\theta_o}{\theta_i}(p)$  in factored form and the transient responses  $\theta_o(t)$  were found. Changes in static margin, autopilot gain, Mach number, and altitude were also considered. The major part of the computing was conducted on the Bell Telephone Laboratories X-66744 relay computer at the Langley Laboratory.

The method of adjusting the autopilot gain is demonstrated in reference 2. To determine an autopilot gain, the open-loop frequency response is plotted on the rectangular coordinates, phase against amplitude in decibels. A typical chart used for this purpose is shown in figure 2. The set of coordinates superimposed on figure 2 are curves of constant magnitude in decibels and constant phase of the closed-loop system. The open-loop response curve is then shifted up or down until it is tangent to the closed-loop constant-magnitude curve of 2.28 decibels. The shift of the open-loop response curve until it is tangent to the closed-loop constant-magnitude curve of 2.28 decibels means that the closed-loop frequency response will have a peak amplitude ratio of 1.3. The amount of vertical shift of the open-loop frequency-response curve gives the autopilot gain of the system in decibels. This means that the autopilot gain is determined with respect to the amplitude ratio of the closed-loop frequency response. An ideal closed-loop frequency response is represented by the zero-decibel curve (amplitude ratio 1.0) and could be used for selecting the autopilot gain by attempting to make the open-loop frequency response follow it. However, the method of selecting the open-loop gain with respect to the peak of the closed-loop frequency response was used. The gain factor thus determined was then used to compute the response of the system at all conditions of Mach number and altitude. The convenience of the phase-magnitude plot is that both the

open- and closed-loop frequency responses are seen as related quantities and, for a change in the open-loop response, the corresponding change in the closed-loop response is immediately apparent.

## RESULTS AND DISCUSSION

The purpose of this paper is to show the conditions under which it is possible to obtain satisfactory longitudinal performance of a supersonic canard missile configuration. To do this, a series of curves were calculated for various conditions of Mach number, altitude, and static margin and those which adequately summarize the results are presented.

### Missile Longitudinal Performance

Perhaps the most significant performance curve of an automatically controlled missile is the response to a step-input disturbance. While such an input may never appear when the missile is used as part of a guidance system, examination of this transient response allows a great many of the performance qualities to be deduced. In order to obtain this response, the step input is applied so that the reference of the attitude gyroscope (if an attitude control system is under consideration) is displaced. This causes the autopilot to produce a control-surface deflection of the proper sign so that the airframe will assume the new attitude angle.

For the transient responses presented herein, a zero-lag autopilot was assumed. This is a reasonable assumption since such an autopilot has been tested in flight as described in reference 1, and several hydraulic systems have been developed with a flat amplitude and zero phase characteristic to 40 cycles per second, as described in reference 5.

A satisfactory response is considered to be one which closely follows the step input. There are several reasons for using this as a criterion. If the output does not closely follow the input, the homing phase of a flight may be inaccurate. An oscillatory response requires a large amount of energy to keep the necessary servos acting. This, in turn, means that the bulk of the missile must be sufficiently large to contain the necessary batteries or air supply. Increasing the size of the missile means that both mass and aerodynamic drag will be increased so that a larger propulsion system must be used to provide specified accelerations.

Figure 3 is a closed-loop transient response in  $\theta$  for the missile with a large static margin, approximately 0.86c, at Mach number 1.8. This response is considered slow. When the autopilot gain  $K_A$  was

adjusted, as explained in the analysis, the resulting response was shown to be slower yet. However, the amplitude of oscillation has been decreased. To increase the speed of response, the static margin was decreased to approximately 0.14c. Figure 4 shows the resulting responses for the system with and without autopilot gain adjustment. The autopilot gain adjustment acted to decrease the speed of response. With no autopilot gain adjustment  $\theta_0$  reaches the step-input value in less than 0.1 second, but because of the high amplitude and high frequency of the oscillations the response is not considered satisfactory.

Because satisfactory performance was not obtained from the missile system alone, a control system to provide damping was introduced. This control system was assumed to act like a spring mass system with damping and to provide control deflections proportional to the rate of pitch  $\dot{\theta}$  of the missile. Figure 5 shows the curves obtained when the proposed rate control was assumed to be acting on the canard fin control surfaces and the missile had a large static margin. By comparing these curves with those of figure 3, the additional damping is apparent; however, the speed of response is not appreciably increased even with the autopilot gain adjusted. Therefore, the static margin was decreased and figure 6 shows how the response characteristics were improved. At sea level and Mach number 1.8, with an autopilot gain of 1, the output attains 63 percent of the input in 0.1 of a second and there is no oscillation present. The response time increases with decreasing Mach number and oscillations begin to appear only for Mach numbers below 1.2. Satisfactory responses were also obtained for the altitudes considered. The response at 40,000 feet and Mach number 0.8 is relatively slow and oscillatory, but this is not considered to be serious in view of the improved performance obtained at other Mach numbers and altitudes. The autopilot gain was then adjusted according to the method given in the analysis, and at sea level and Mach number 1.8  $K_A$  was found to be about 2.7. Because the speed of response obtained with this gain adjustment was increased, responses showing the effect of altitude and Mach number with the same  $K_A$  were made. These curves are also presented in figure 6. The autopilot gain adjustment acts to increase the speed of response and is accompanied by an increased amount of oscillation. The conclusion reached from these transient curves is that satisfactory performance of the missile can be obtained from the missile with a small static margin throughout the Mach number and altitude range considered, providing the proposed rate control is used.

#### Selection of Rate Factor

The rate factor or rate gyro sensitivity was initially selected on the basis of experience with similar equipment and calculations begun using  $K_r = 518$  when the rate control was assumed to be acting on the

canard-fin control surfaces. Later it was decided to determine how critical the rate factor might be in obtaining satisfactory system performance. This was done by obtaining experimental frequency-response data from a scale model of the missile configuration as it became available and combining it with the theoretical rate-control data. Then, using several different values for the rate factor  $K_r$ , frequency responses were plotted on a phase-magnitude chart as shown in figure 7. Note that these data are for one value of altitude, Mach number, and static margin. Also, the zero-decibel (amplitude ratio 1.0) closed-loop contour is shown for reference, the remaining closed-loop contours being omitted for purposes of clarity. Curves are looked for which can be made to follow the closed-loop zero-decibel contour closely without passing inside the 2.23-decibel closed-loop contour. The two curves in figure 7 for which this might be possible are those which have the rate factors 550 and 700. The manner of shifting the frequency-response curve, which amounts to adjusting the autopilot gain, is demonstrated in figure 8. The open-loop frequency response has been shifted up approximately 12 decibels corresponding to  $K_A = 4$ . Considering the differences in conditions between this system and the system in the main body of the paper, with respect to both conditions and methods, the discrepancy between this gain adjustment and the gain adjustment of figure 6 is considered not to be unreasonable. The closed-loop frequency response was then read directly from the plot and the transient response was computed from this frequency response using a Fourier series, as explained in reference 6. Figures 9 and 10 are the transients obtained from applying a Fourier series to a closed-loop frequency response for the system when the rate factor is 550 and 700, respectively. The fact that the curve of figure 9 does not reach steady state is attributed to the method of obtaining it. The change in value of the rate factor from 550 to 700 does not affect the transient response seriously. Therefore, the conclusion is drawn that the rate factor can assume a fairly wide range of values without appreciably affecting the system transient response. Figure 7 shows that the frequency distribution along the curves does not change appreciably by changing the rate factor between 550 and 700. Therefore, having considered both the transient and frequency responses, the conclusion was reached that the estimated rate factor as used in the system analysis is reasonable.

The rate-control-system parameters  $\zeta$ , the damping ratio, and  $\omega_n$ , the natural frequency, were selected on the basis of experience as with the rate factor. Note that the natural frequency 88 radians per second as chosen is beyond any natural frequency anticipated from the missile alone and that for the value of  $\zeta$  chosen the  $\frac{\delta r}{\theta}$  frequency response is reasonably flat out to its natural frequency. Figure 11 shows an experimental curve obtained for a rate gyro-servo combination under a spring load. This response revealed that the specified control system

is physically realizable because a frequency response for  $\frac{\delta r}{\dot{\theta}}$  obtained from this curve by the method given in reference 6 had a natural frequency of 88 radians per second and a damping ratio of 0.4.

### Angle of Attack and Normal Acceleration

A few transient calculations were made for angle of attack and normal acceleration. These were done for sea-level conditions at Mach number 1.8 with and without rate control. Figure 12(a) corresponds to the  $\theta_0$  response shown in figure 4 for  $K_A = 1.0$  and figures 12(b) and 12(c) correspond to the  $\theta_0$  responses of figure 6 for  $K_A = 1.0$  and  $K_A = 2.7$ , respectively, at sea level and Mach number 1.8. The figures show that the same heading change can be accomplished by the missile with a smaller maximum angle of attack and normal acceleration when the proposed rate control is included. This means that greater heading changes can be called for without exceeding the structural limitations of the missile if the system has auxiliary damping.

### Frequency Response

The open-loop frequency response of the configuration was plotted as Nyquist diagrams for various conditions and the resulting curves are shown in figures 13 to 18. Figure 13 shows the missile response for two Mach numbers when the static margin is 0.86c and there is no rate control in the system. The curve for Mach number 1.8 of figure 13 corresponds to the transient response of figure 3 where  $K_A = 1$ . Figure 14 shows the missile response for two Mach numbers when the static margin is 0.14c and there is no rate control in the system. The curve for Mach number 1.8 of figure 14 corresponds to the transient response of figure 4 where  $K_A = 1$ . Because the shapes of the Nyquist diagrams remain the same regardless of Mach number and static-margin changes, there is no reason to expect that changes in these parameters can improve the performance of the missile without some auxiliary kind of control. According to reference 7 an ideal frequency response corresponding to a zero error displacement system is represented on a Nyquist diagram by a vertical line projecting downward with infinite frequency at the origin. Figure 15 shows the frequency response for the missile when rate control is included in the system, and corresponds to the transients of figure 5 with  $K_A = 1$ . The Nyquist diagrams do not show any reasonable approach to the type of frequency response required for an ideal zero error displacement system, indicating that satisfactory transient qualities could not be expected. However, with a decrease in static margin a considerable improvement in curve shape is obtained, as can be seen in figures 16 to 18. These Nyquist diagrams are the open-loop frequency responses corresponding to the transient responses of

figure 6 when  $K_A = 1$ . As can be expected, the curve shapes depart further from the ideal with increasing altitude.

From the comparisons obtained between the closed-loop transient responses and the open-loop frequency responses, the conclusion is reached that the conventional method of using the Nyquist diagrams for system stability analysis is useful for preliminary study. For the missile system of this paper it revealed the change in shape of the frequency response due to the combination of small static margin and rate control that produced satisfactory system performance.

### Pole Plots

The analysis used in this paper is centered primarily on the methods of Laplace which reduce the differential equations of motion of the missile to algebraic functions. The denominator of these functions has a number of roots depending on its degree, and these roots are called poles. Pole plots proved useful for preliminary examination of the system response characteristics. The position of the poles in the complex plane determines characteristics such as damping and frequency. Figure 19 is a plot for the missile without rate control for two static margins at sea-level conditions showing the effects of Mach number. With an increase in Mach number the natural frequency and damping increase, and with a decrease in static margin the natural frequency and damping decrease.

Figures 20(a) to 20(d) are pole plots for  $\frac{\theta_0}{\theta_1}(p)$  of the missile when rate control is present in the system. The presence of the additional mode of motion due to the inclusion of rate control is now noted, the points high in the plane being attributed to the rate-control system and those lower in the plane being attributed to the airframe. One real pole is also shown on the plot. That real pole is the one which is farthest to the right for the Mach number range considered. In the cases shown it corresponds to Mach number 0.8.

Note how the poles for the rate gyro move to the right while those of the airframe move to the left with increasing Mach number. A consequence of this is that at sea-level conditions the natural frequency of the rate-control system becomes dominant above a Mach number of approximately 1.2, as can be seen in figures 20(a) and 20(b). Dominance of a pole is demonstrated mathematically in reference 8. This effect is no longer present, however, at 10,000 feet and 40,000 feet, as can be seen from figures 20(c) and 20(d).

The most significant consequence of introducing artificial damping is readily seen in these pole plots. That is, the complex poles of the

airframe now lie much farther to the left of the frequency axis, demonstrating the increased damping in the missile. Also, the real poles which signify the presence of the simple time lag of the missile response are relatively unaffected, as can be seen by comparing figure 19 with figures 20(a) and 20(b). This means that, even though damping has been introduced into the missile, the speed of response remains about the same.

A study of the pole plots of the system showed that a large amount of information can be condensed into a single plot and performance characteristics determined for a wide variation of parameters without making any transient calculations. The pole plots illustrate the presence of the additional mode of motion which rate control added to the system.

### Tip Control

Damping as discussed herein was introduced into the missile through the canard fins. Consideration was also given to the use of wing-tip elevators for the damping. When this was done, the sensitivity  $K_r$  of the rate gyro was set so that the aerodynamic moment obtained from the tip elevators would be the same as when the damping was introduced through the canards at Mach number 1.8 and sea-level conditions. The results were that approximately the same performance can be obtained by introducing the proposed control through the wing-tip elevators, since the variation of pitching-moment coefficient for tip elevators and canard fins against Mach number is nearly identical.

### CONCLUDING REMARKS

A theoretical analysis was conducted to determine the dynamic performance characteristics of an automatically controlled supersonic canard missile configuration. The object of the investigation was to show the means which might be used to improve the performance qualities of the missile for possible guidance applications. The longitudinal frequency-response and transient-response characteristics were calculated from the differential equations of motion of the system, assuming two degrees of freedom. The unsatisfactory performance qualities were attributed largely to a lack of inherent aerodynamic damping. Therefore, the damping was increased through a proposed control system which consisted of a rate gyro-servo combination. This device acted through the wing-tip elevators or canard fins to produce a control deflection proportional to the rate of pitch of the missile.

The conclusion is reached that when the rate control is included in the missile, satisfactory system performance is obtained throughout

the Mach number and altitude range considered when the static margin is small. The performance was improved with respect to the attitude, normal acceleration, and angle-of-attack response. Because the auxiliary damping improved the response of the system with respect to angle of attack and normal acceleration, greater heading changes can be called for without exceeding the structural limitations of the missile.

Certain remarks can be made concerning the analysis. The rate factor used and the method of adjusting the gain of the autopilot permitted satisfactory performance to be obtained. The procedure used to obtain frequency-response and transient-response characteristics is simple and direct. Nyquist diagrams were useful for system-stability analysis. The manner in which the small static margin and rate control change the shape of the Nyquist diagram to produce good system performance is shown. Pole plots were useful for examining the response characteristics throughout the variation of conditions considered. Also, they illustrated the presence of the additional mode of motion due to the rate of gyro control system.

Langley Aeronautical Laboratory  
National Advisory Committee for Aeronautics  
Langley Air Force Base, Va.

## REFERENCES

1. Gardiner, Robert A., and Zarovsky, Jacob: Rocket-Powered Flight Test of a Roll-Stabilized Supersonic Missile Configuration. NACA RM L9K01a, 1950.
2. Brown, Gordon S., and Campbell, Donald P.: Principles of Servomechanisms. John Wiley & Sons, Inc., 1948.
3. Churchill, Ruel V.: Modern Operational Mathematics in Engineering. McGraw-Hill Book Co., Inc., 1944.
4. Bode, Hendrik W.: Network Analysis and Feedback Amplifier Design. D. Van Nostrand Co., Inc., 1945.
5. Bassett, L. F.: Missile Guidance and Control. Part III - Application of the Integrating Gyro to Guided Missile Roll Stabilization. Instrumentation Lab., M.I.T. Thesis, 1949.
6. Seamans, Robert C., Jr., Bromberg, Benjamin G., and Payne, L. E.: Application of the Performance Operator to Aircraft Automatic Control. Jour. Aero. Sci., vol. 15, no. 9, Sept. 1948, pp. 535-555.
7. Hall, Albert C.: The Analysis and Synthesis of Linear Servomechanisms. The Technology Press, M.I.T., 1943.
8. Mulligan, J. H., Jr.: The Effect of Pole and Zero Locations on the Transient Response of Linear Dynamic Systems. Proc. I.R.E., vol. 37, no. 5, May 1949, pp. 516-529.

TABLE I

## ESTIMATED DERIVATIVES VERSUS MACH NUMBER

[Static margin = 0.14c at  $M = 1.8$ .  
All derivatives in radian measure]

Mach number	$C_{L\alpha}$	$C_{m\alpha}$	$C_{mq}$	$C_{m\dot{\alpha}}$	$C_{L\delta_s}$	$C_{m\delta_s}$	$C_{L\delta_t}$	$C_{m\delta_t}$
0.8	3.5195	-0.2192	-11.457	-0.651	-0.0632	1.2230	0.3152	-0.3894
1.0	4.1213	-.4197	-14.607	-1.132	-.1675	1.5731	.3770	-.4745
1.2	4.3103	-.8737	-14.660	-1.007	-.1000	1.4387	.3553	-.4500
1.4	3.9662	-.7140	-13.254	-.838	-.0602	1.2739	.3215	-.4072
1.6	3.6876	-.5851	-12.134	-.707	-.0271	1.1420	.2951	-.3738
1.8	3.4866	-.5024	-11.303	-.609	-.0029	1.0427	.2725	-.3452



TABLE II

## ESTIMATED DERIVATIVES VERSUS MACH NUMBER

[Static margin = 0.86c at  $M = 1.8$ .  
All derivatives in radian measure]

Mach number	$C_{L\alpha}$	$C_{m\alpha}$	$C_{mq}$	$C_{m\dot{\alpha}}$	$C_{L\delta_s}$	$C_{m\delta_s}$	$C_{L\delta_t}$	$C_{m\delta_t}$
0.8	3.5195	-2.8145	-19.967	-2.270	-0.0632	1.2686	0.3152	-0.6139
1.0	4.1213	-3.3707	-25.574	-3.623	-.1675	1.6934	.3770	-.7450
1.2	4.3103	-3.9601	-26.549	-3.149	-.1000	1.5104	.3553	-.7048
1.4	3.9662	-3.5580	-23.985	-2.622	-.0602	1.3171	.3215	-.6379
1.6	3.6876	-3.2292	-21.924	-2.212	-.0271	1.1614	.2951	-.5855
1.8	3.4866	-2.9972	-20.430	-1.906	-.0029	1.0447	.2725	-.5406



TABLE III  
VELOCITY AND DYNAMIC PRESSURE VERSUS MACH NUMBER  
AT VARIOUS ALTITUDES

Mach number	V			q		
	Sea level	10,000 ft	40,000 ft	Sea level	10,000 ft	40,000 ft
0.8	892.8	860.8	776.8	947.7	650.6	175.6
1.0	1116	1076	971	1481	1017	274.4
1.2	1339.2	1291.2	1165.2	2132	1464	395.1
1.4	1562.4	1506.4	1359.4	2902	1992	537.8
1.6	1785.6	1721.6	1553.6	3791	2602	702.4
1.8	2008.8	1936.8	1747.8	4799	3294	888.9



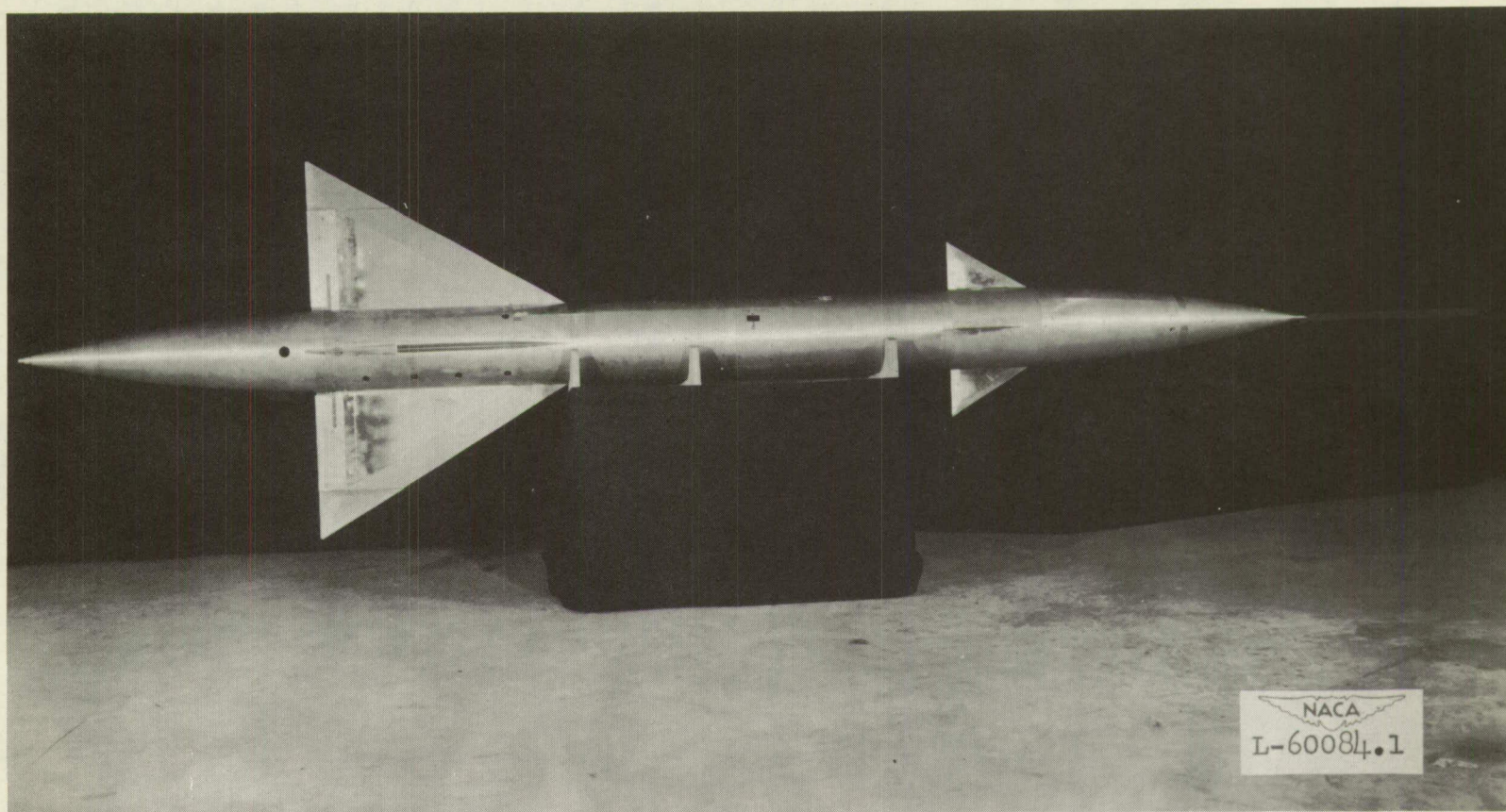


Figure 1.- Photograph of missile configuration.

**Page intentionally left blank**

**Page intentionally left blank**

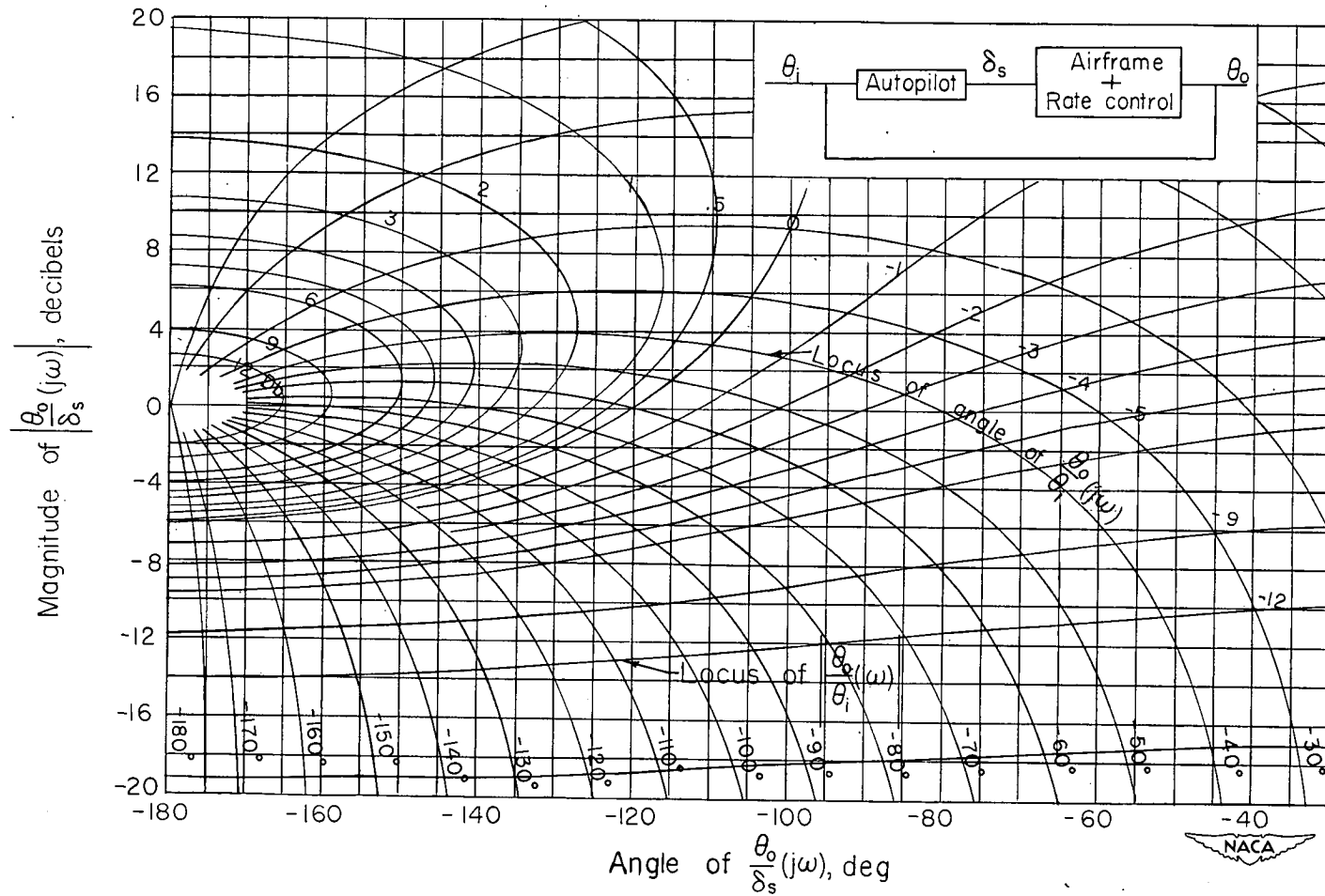


Figure 2.- Chart of open-loop phase angle  $\frac{\theta_o}{\delta_s}(j\omega)$  against open-loop magnitude of  $\frac{\theta_o}{\delta_s}(j\omega)$  showing closed-loop phase contours of  $\frac{\theta_o}{\theta_i}(j\omega)$  and closed-loop magnitude contours of  $\frac{\theta_o}{\theta_i}(j\omega)$ .

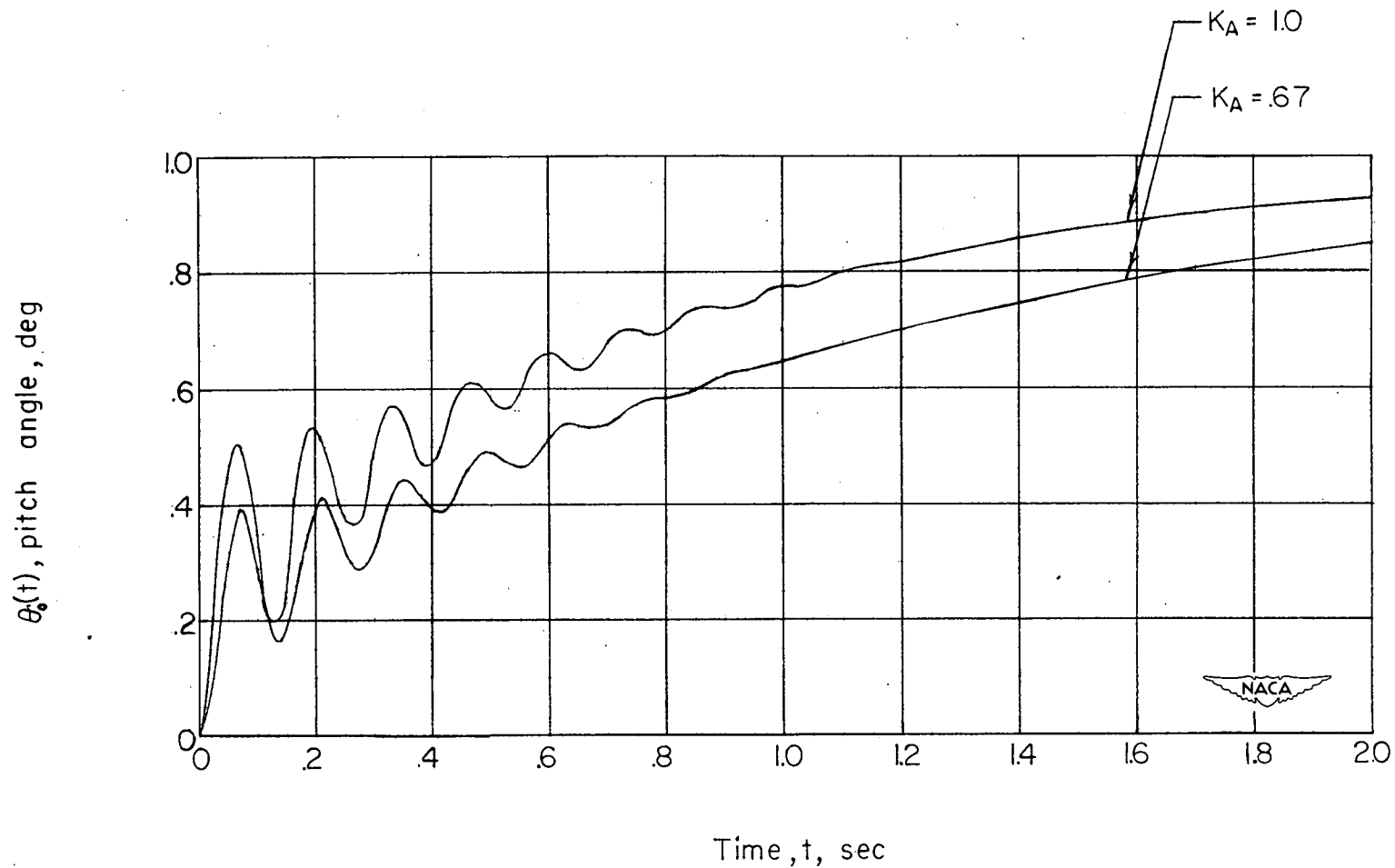


Figure 3.- Longitudinal transient responses  $\theta_o(t)$  of the missile to a unit step input signal calling for a change in attitude of  $1^\circ$ . No additional damping;  $M = 1.8$ ; sea level; static margin =  $0.86c$ .

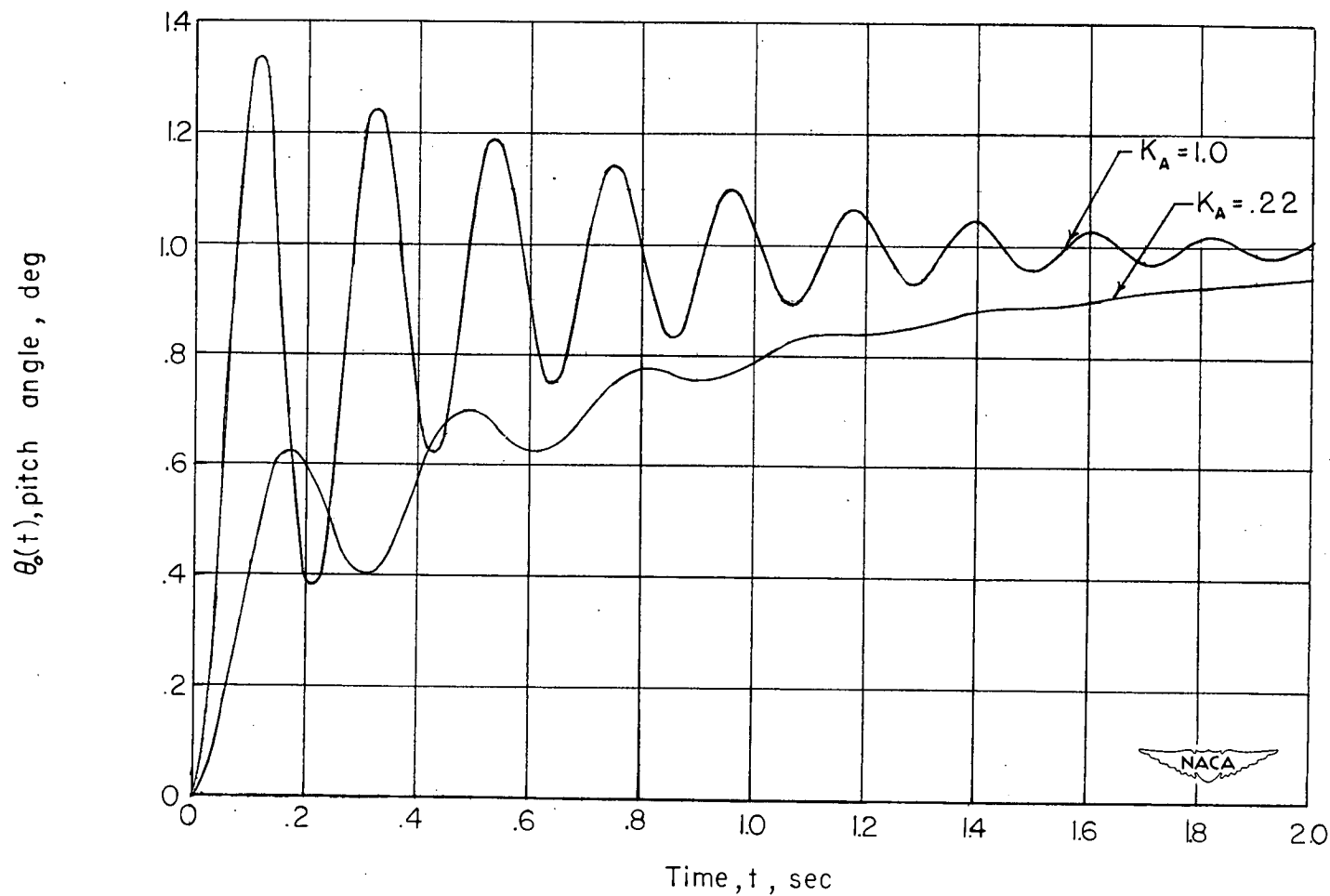


Figure 4.- Longitudinal transient responses  $\theta_0(t)$  of the missile to a unit step input signal calling for a change in attitude of  $1^\circ$ . No additional damping;  $M = 1.8$ ; sea level; static margin =  $0.14c$ .

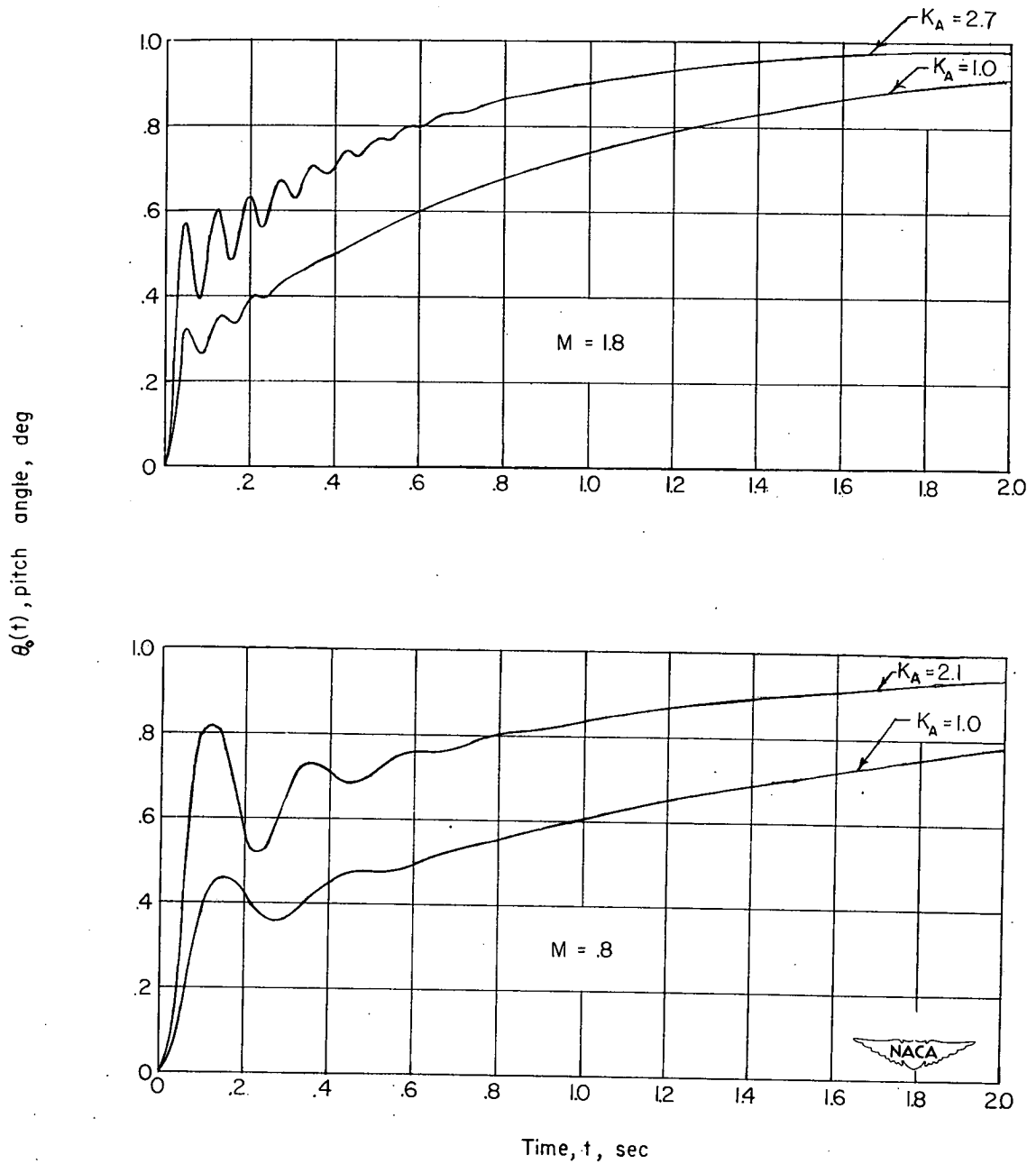


Figure 5.- Longitudinal transient responses  $\theta_0(t)$  of the missile to a unit step input signal calling for a change in attitude of  $1^\circ$ . Auxiliary damping included; sea level; static margin =  $0.86c$ .

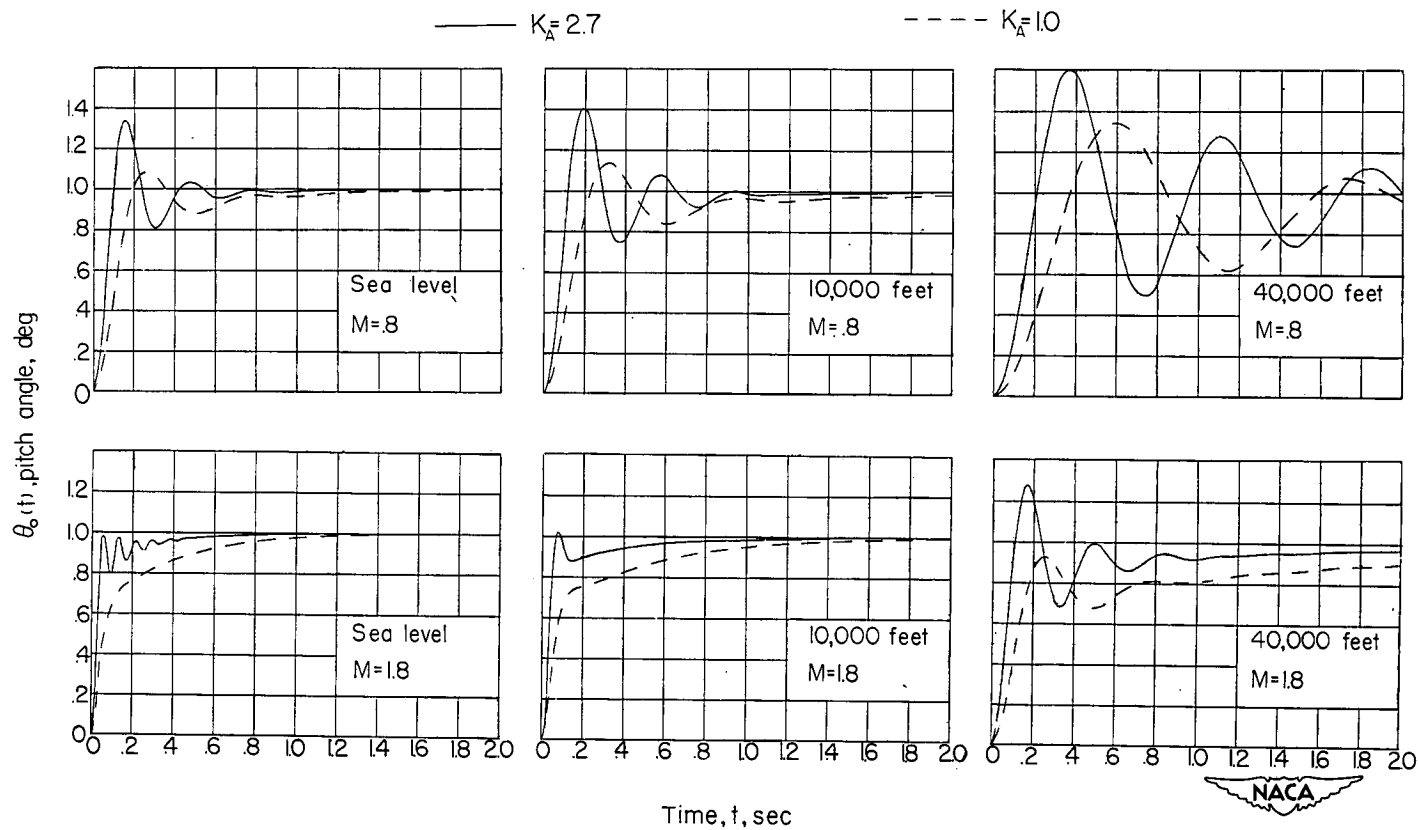


Figure 6.- Longitudinal transient responses  $\theta_o(t)$  of the missile to a unit step input signal calling for a change in attitude of  $1^\circ$ . Auxiliary damping included; static margin = 0.14c.

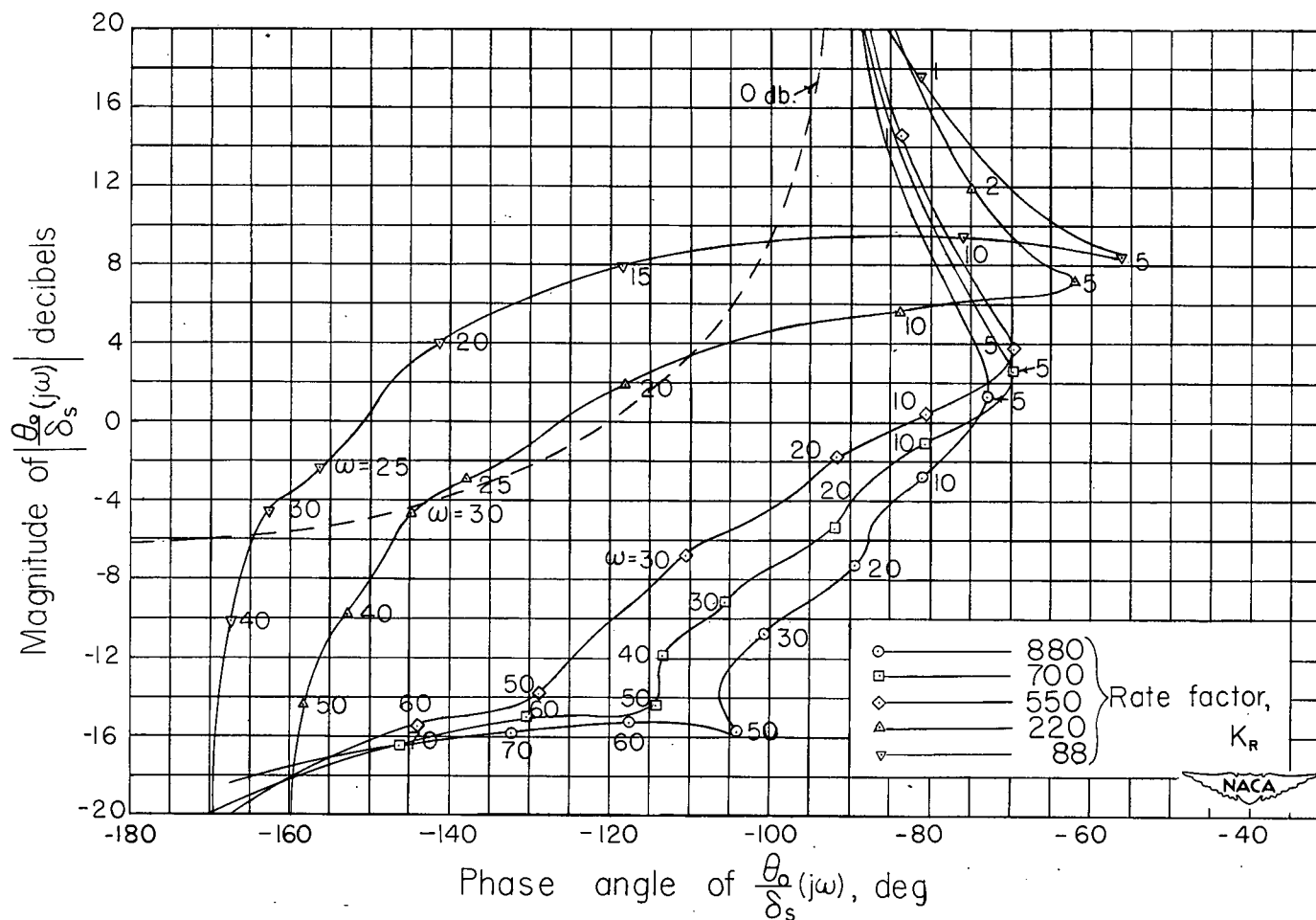


Figure 7.- Longitudinal open-loop frequency-response plot of phase angle against magnitude using experimental missile data with auxiliary damping with several different rate factors. 0 decibel closed-loop contour shown.  $M = 1.3$ ; altitude = 6000 feet; static margin = 0.11c.

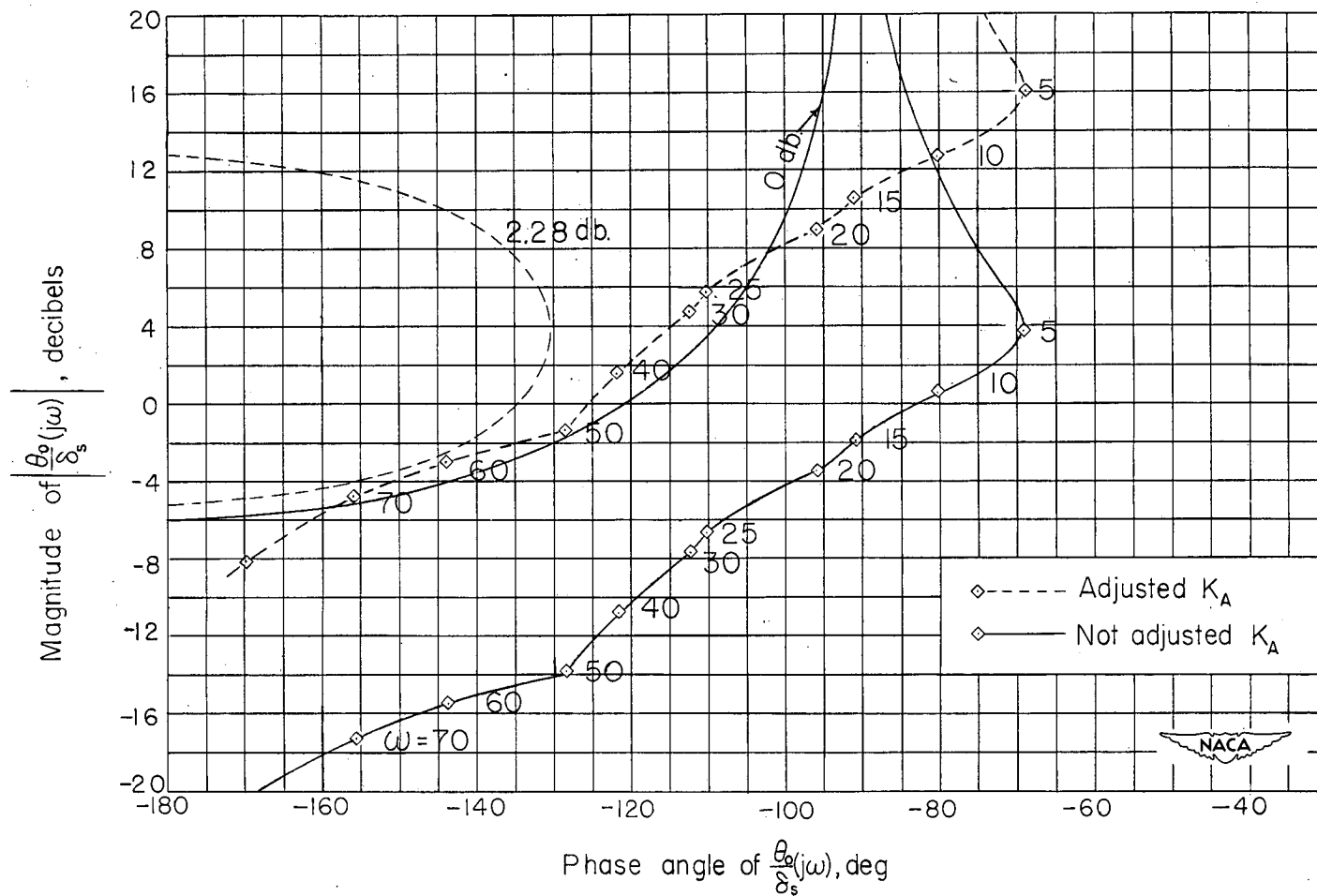


Figure 8.- Adjusted and unadjusted longitudinal frequency-response plots of phase angle against magnitude using experimental missile data with auxiliary damping. 0 decibel and 2.28 decibel contours shown.  $M = 1.3$ ; altitude = 6000 feet; static margin = 0.11c;  $K_T = 550$ .

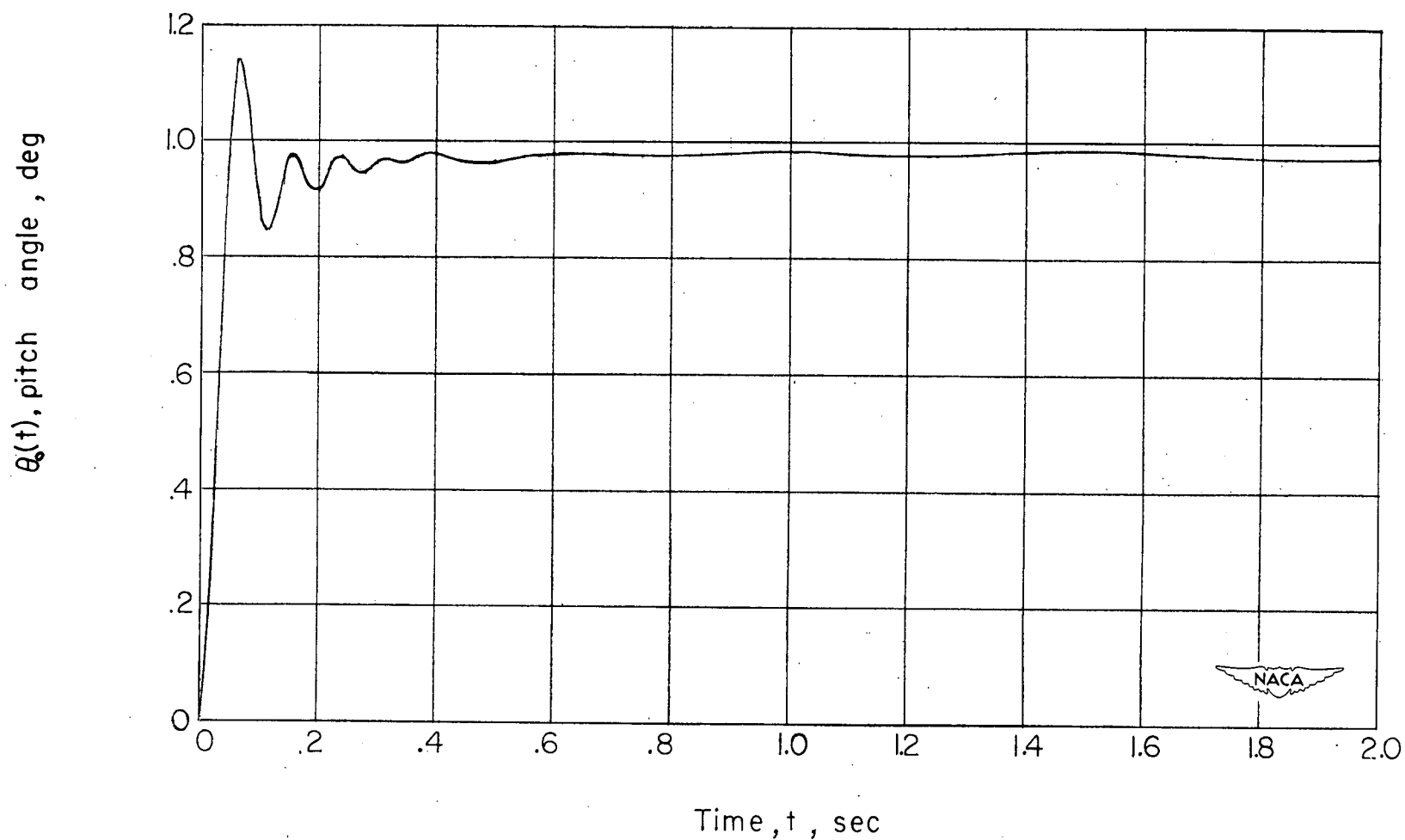


Figure 9.- Longitudinal transient responses  $\theta_0(t)$  of the missile to a unit step input signal calling for a change in attitude of  $1^\circ$ . Additional damping included; experimental missile data used;  $M = 1.3$ ; altitude = 6000 feet; static margin =  $0.112c$ ;  $K_R = 550$ ;  $K_A = 4.0$ .

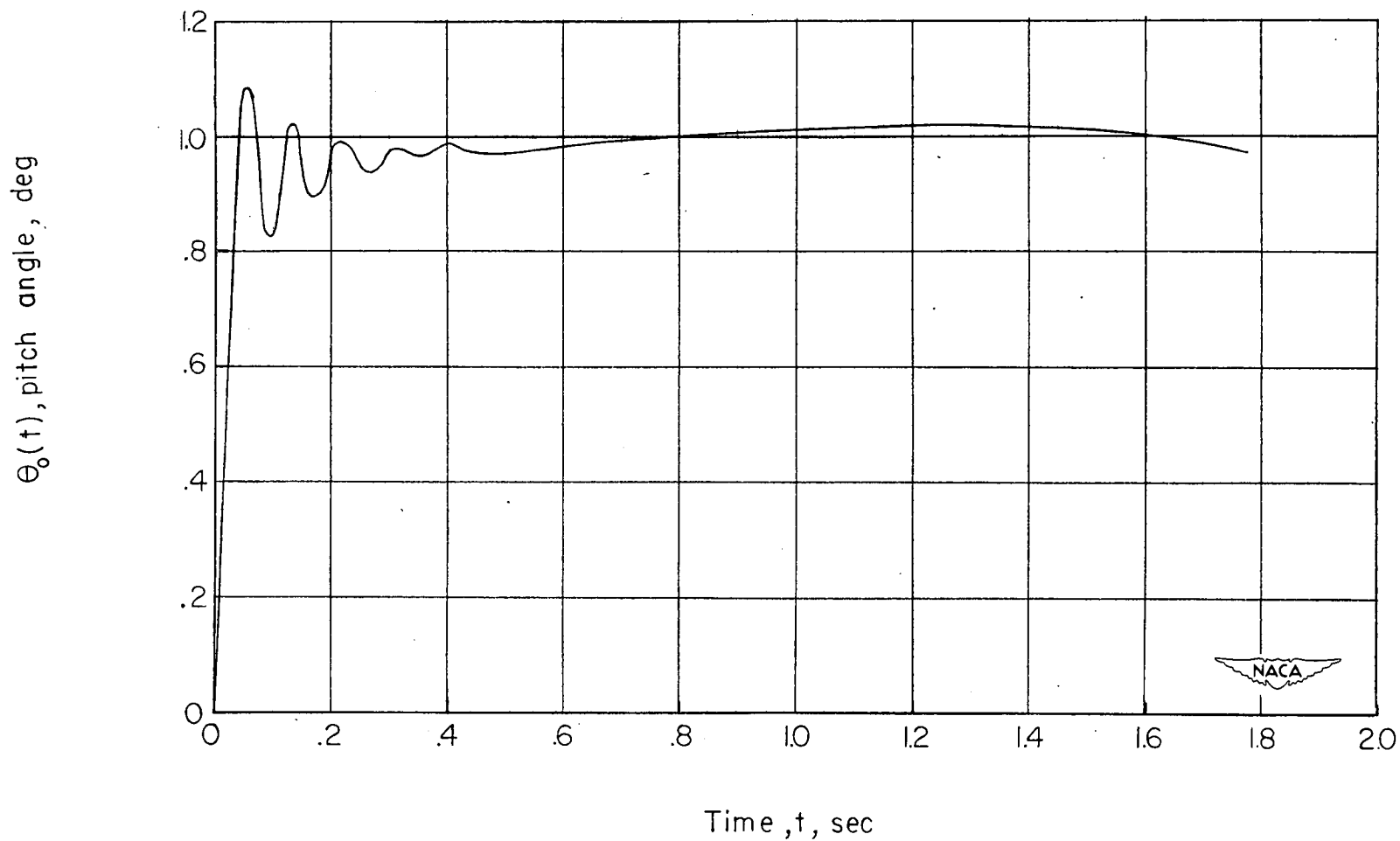


Figure 10.- Longitudinal transient responses  $\theta_o(t)$  of the missile to a unit step input signal calling for a change in attitude of  $1^\circ$ . Additional damping included; experimental missile data used;  $M = 1.3$ ; altitude = 6000 feet; static margin = 0.112c;  $K_R = 700$ ;  $K_A = 4.6$ .

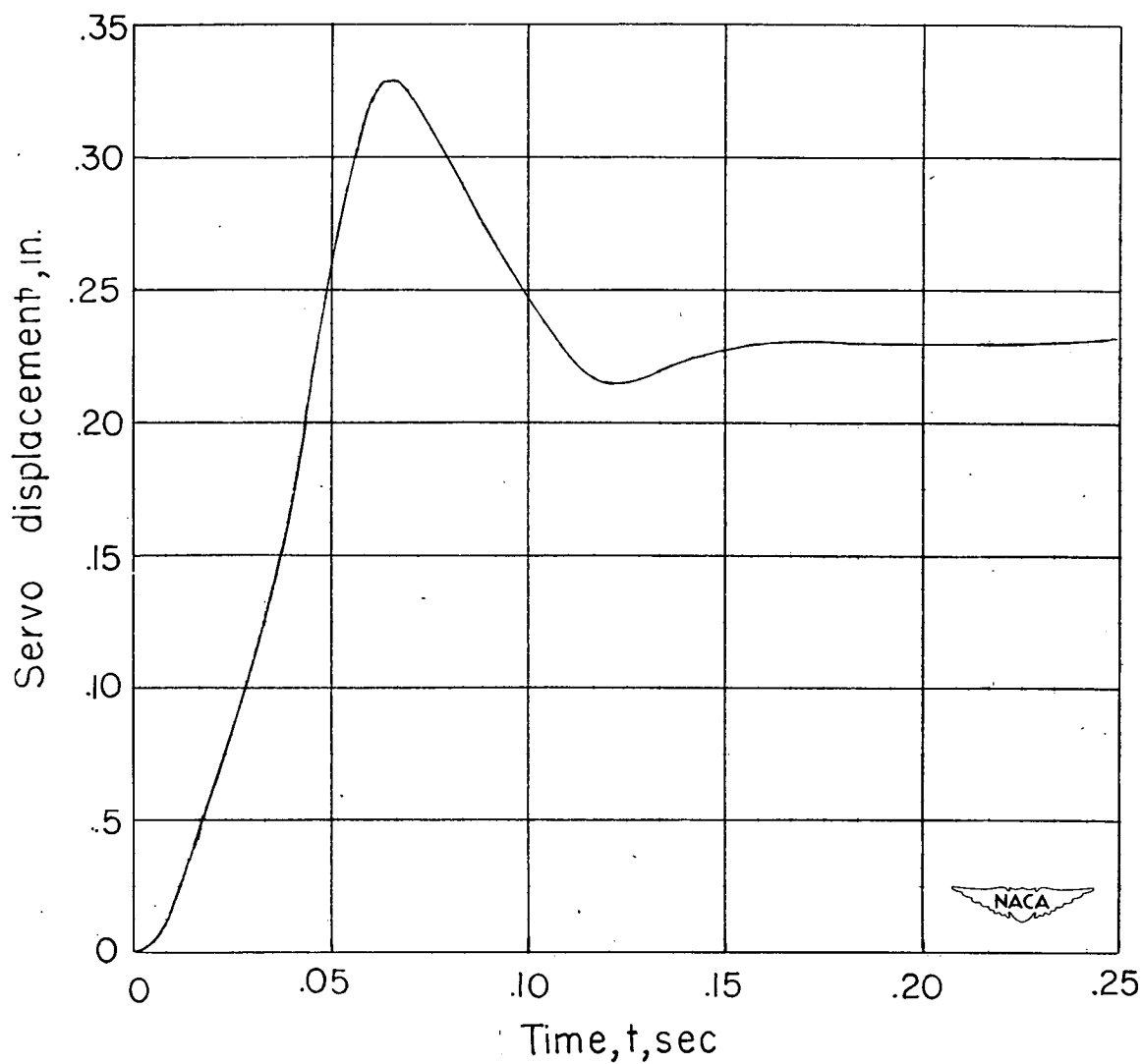


Figure 11.- Experimental transient response of rate gyro system in response to a step deflection of rate gyro gimbal.

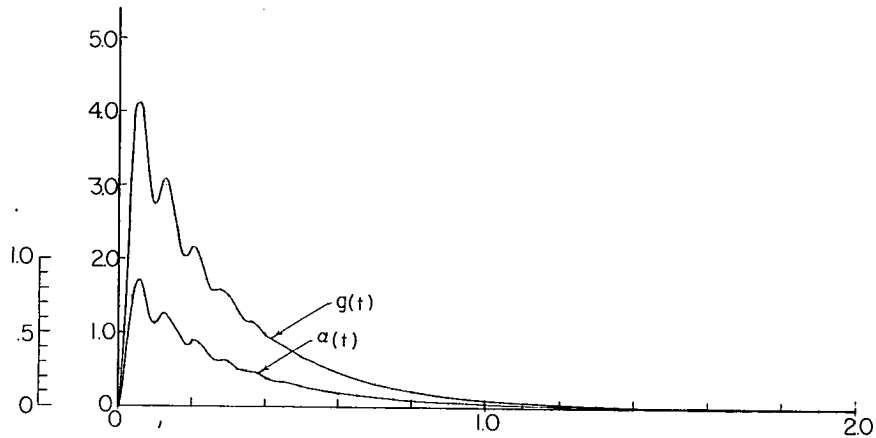
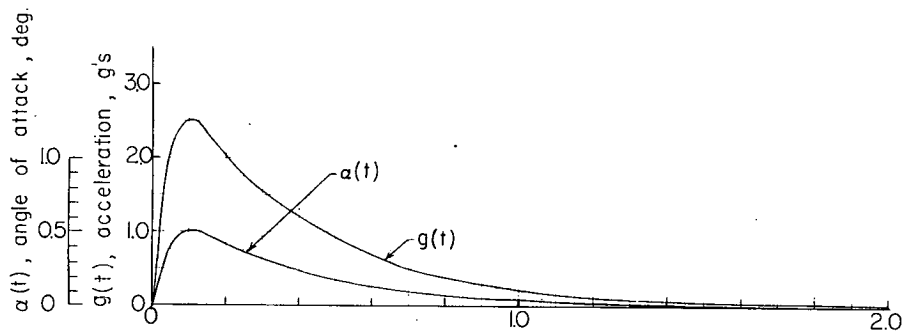
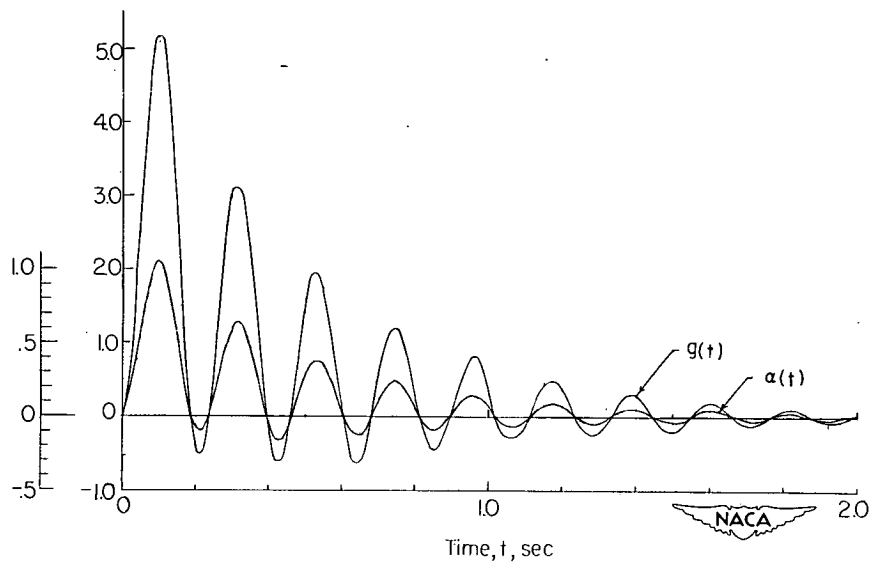
(c) Auxiliary damping  $K_A = 2.7$ .(b) Auxiliary damping  $K_A = 1.0$ .(a) No auxiliary damping  $K_A = 1.0$ .

Figure 12.- Longitudinal transient responses for angle of attack  $\alpha(t)$  and normal acceleration  $g(t)$  of the missile to a unit step input signal calling for a change in attitude of  $1^\circ$ .  $M = 1.8$ ; sea level; static margin =  $0.14c$ .

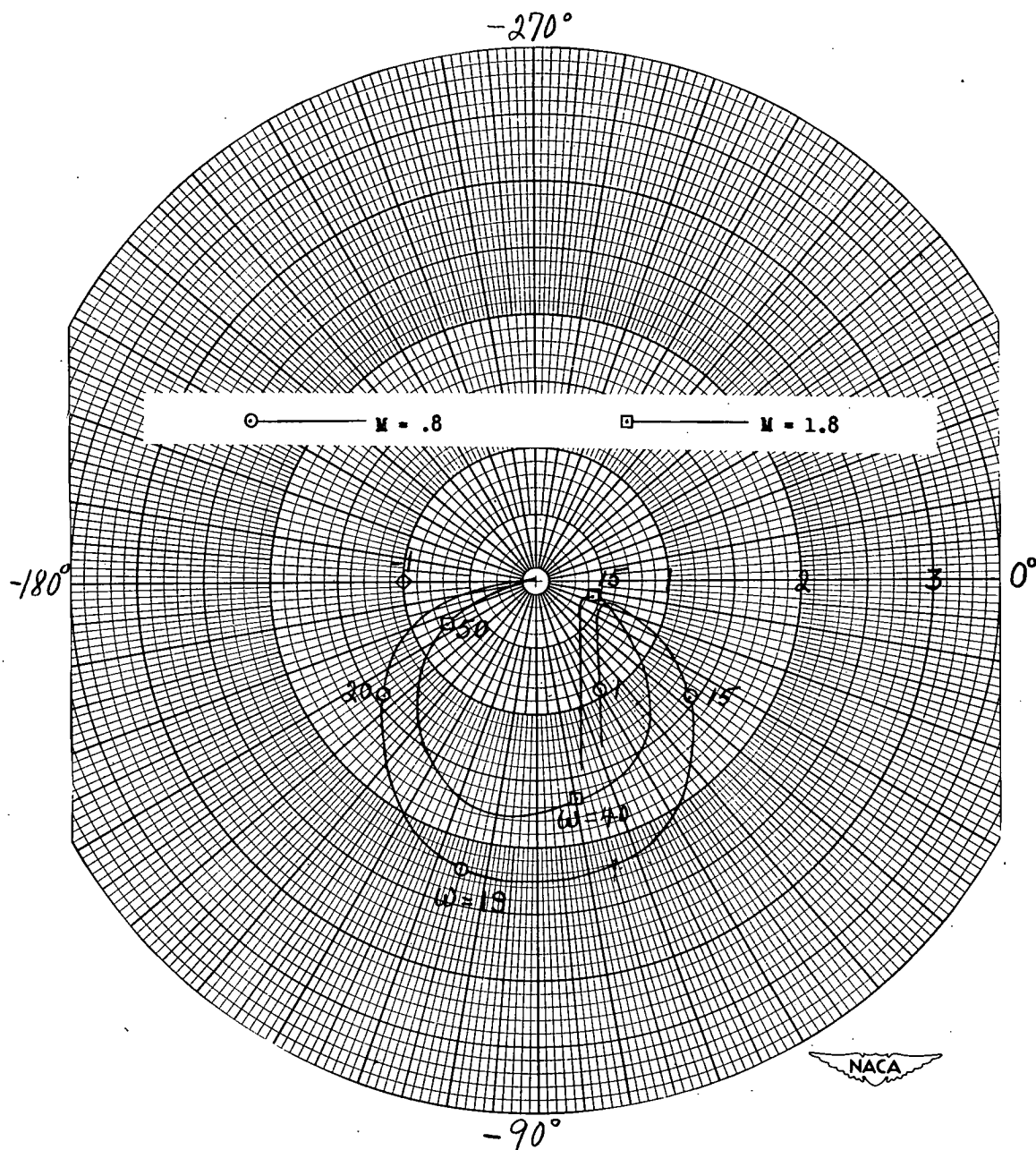


Figure 13.- Nyquist diagram of longitudinal frequency response of missile without additional damping for two Mach numbers showing frequency distribution. Static margin = 0.86c; sea level.

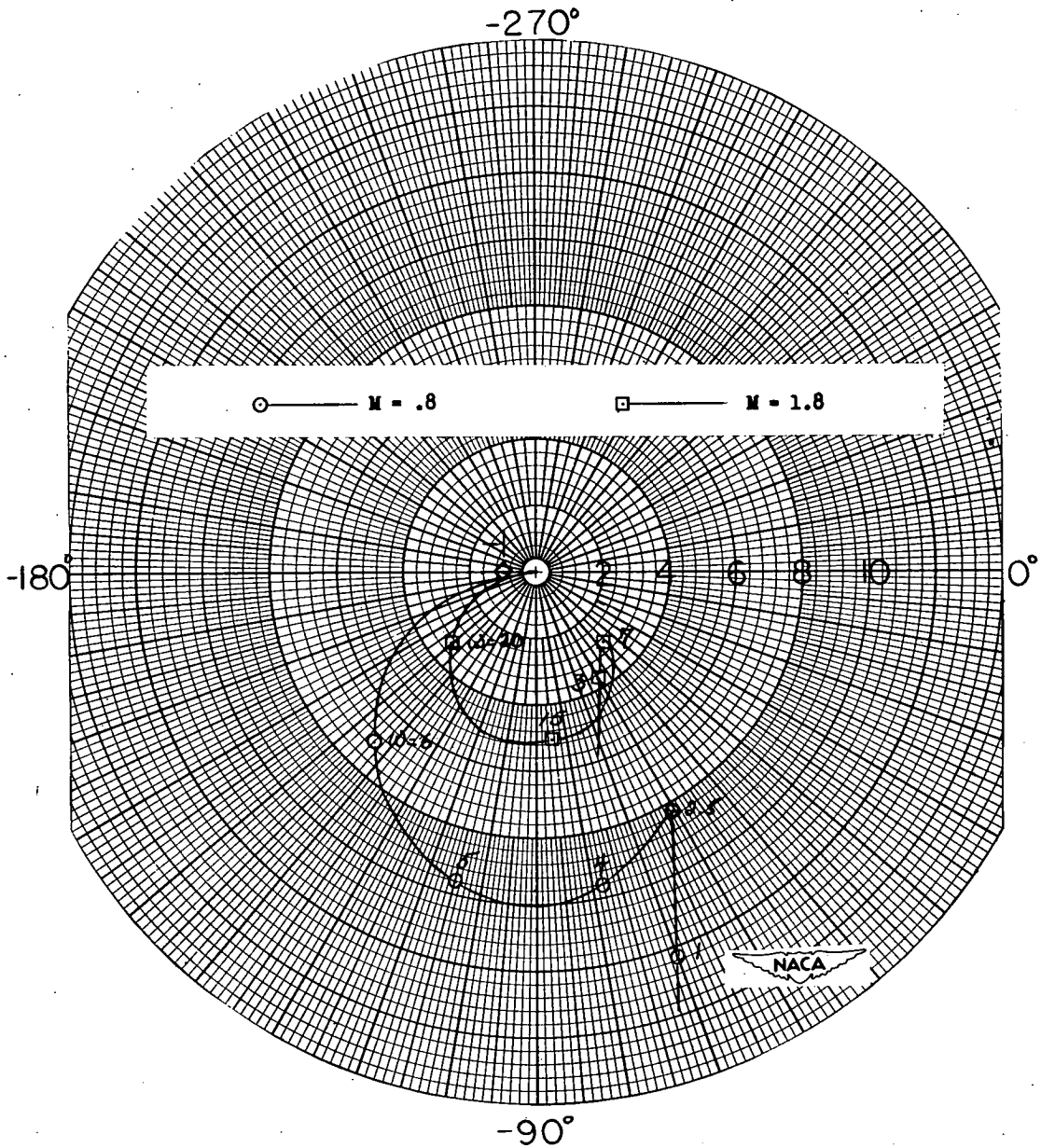


Figure 14.- Nyquist diagram of longitudinal frequency response of missile without additional damping for two Mach numbers showing frequency distribution. Static margin = 0.14c; sea level.

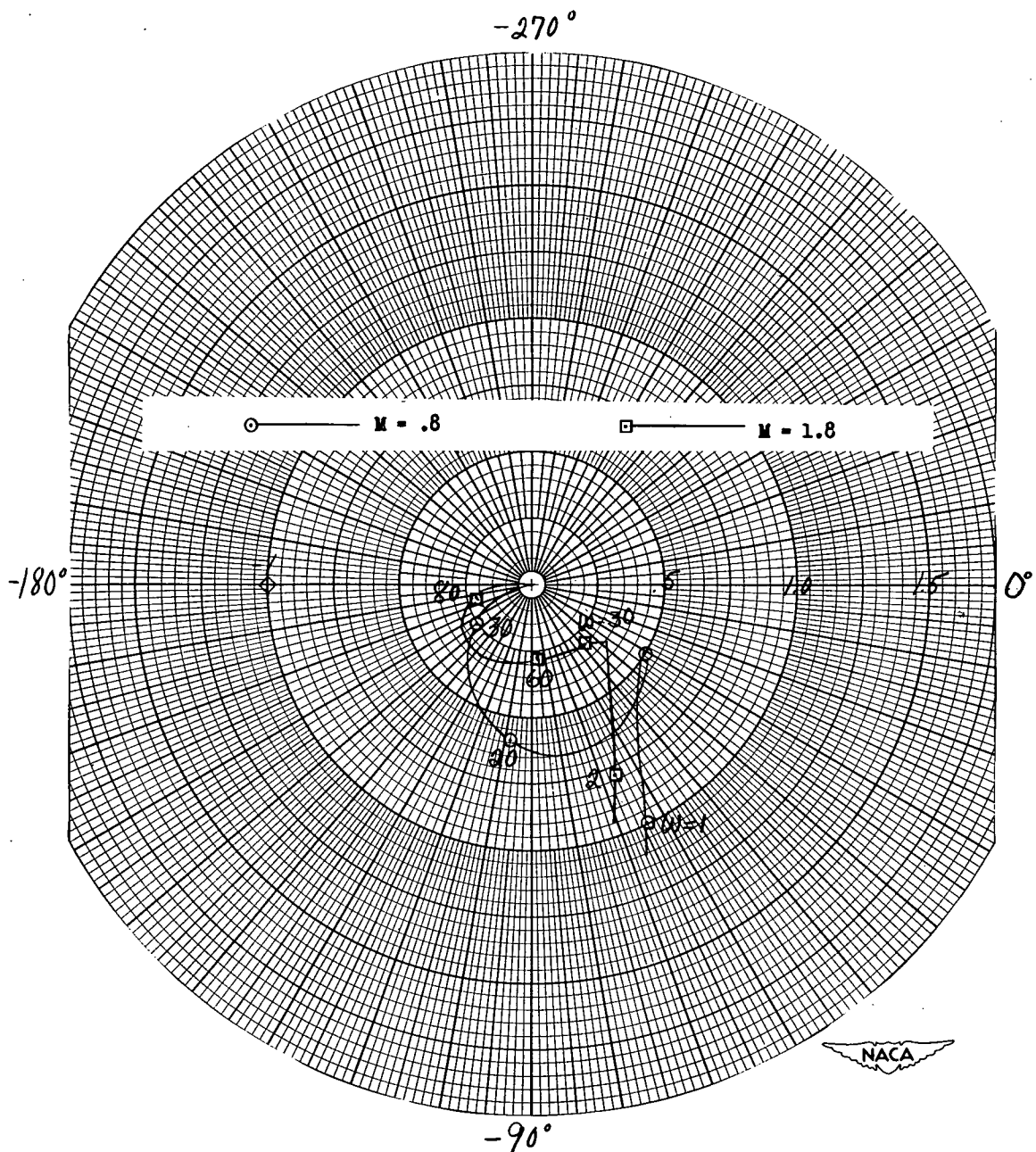


Figure 15.- Nyquist diagram of longitudinal frequency response of missile with additional damping for two Mach numbers showing frequency distribution. Static margin = 0.86c; sea level.

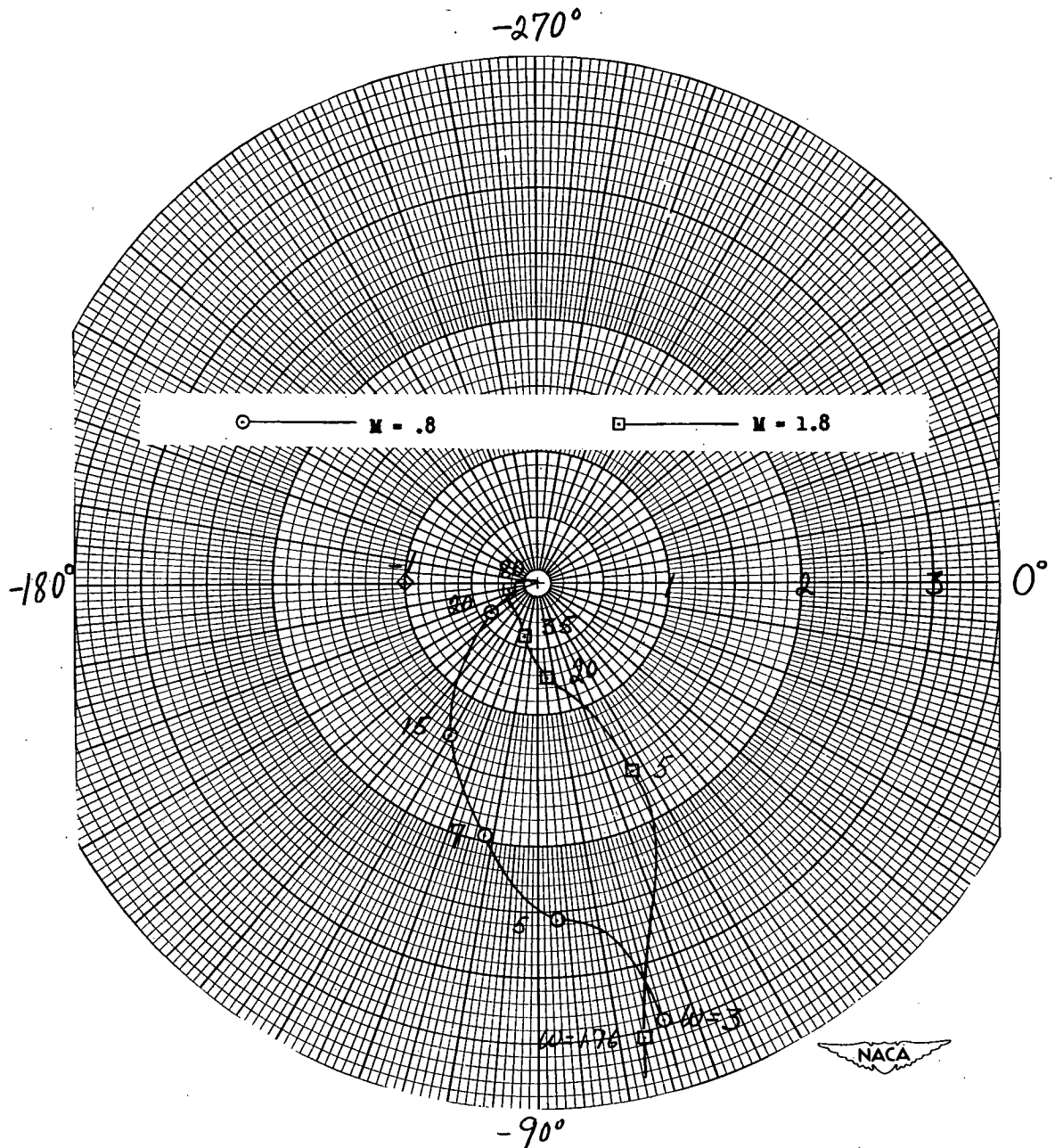


Figure 16.- Nyquist diagram of longitudinal frequency response of missile with additional damping for two Mach numbers showing frequency distribution. Static margin = 0.14c; sea level.

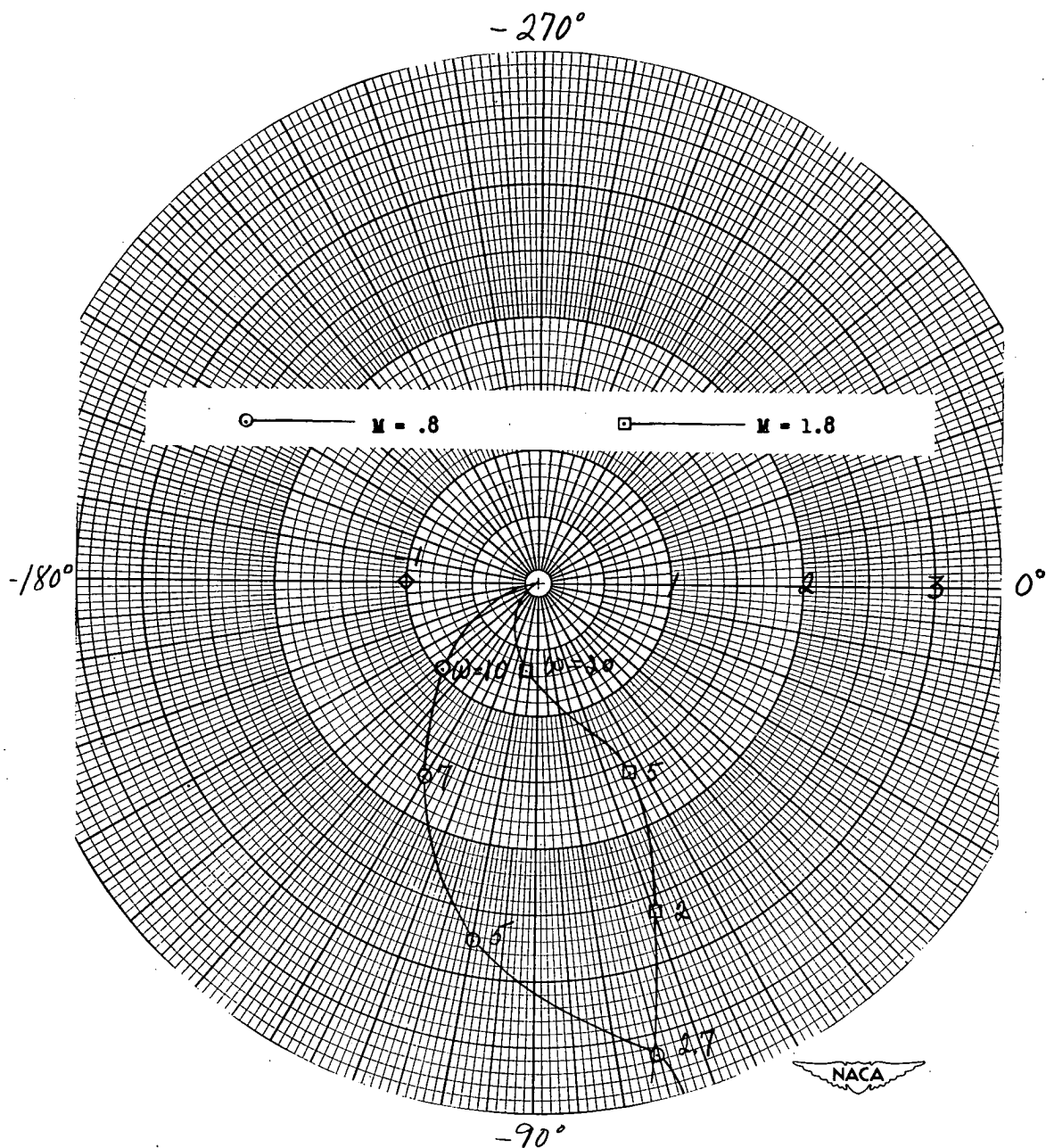


Figure 17.- Nyquist diagram of longitudinal frequency response of missile with additional damping for two Mach numbers showing frequency distribution. Static margin = 0.14c; 10,000 feet.

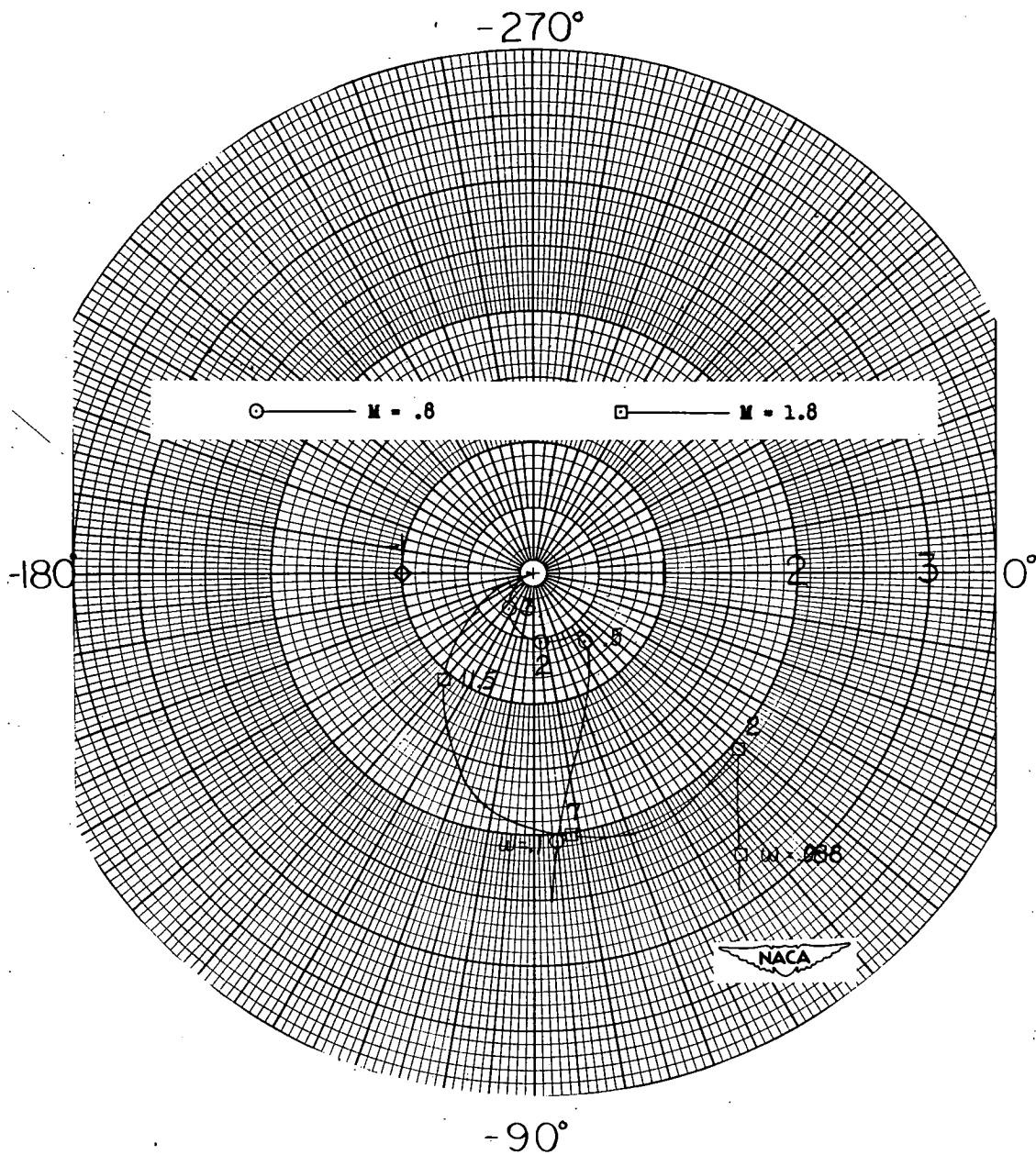


Figure 18.- Nyquist diagram of longitudinal frequency response of missile with additional damping for two Mach numbers showing frequency distribution. Static margin = 0.14c; 40,000 feet.

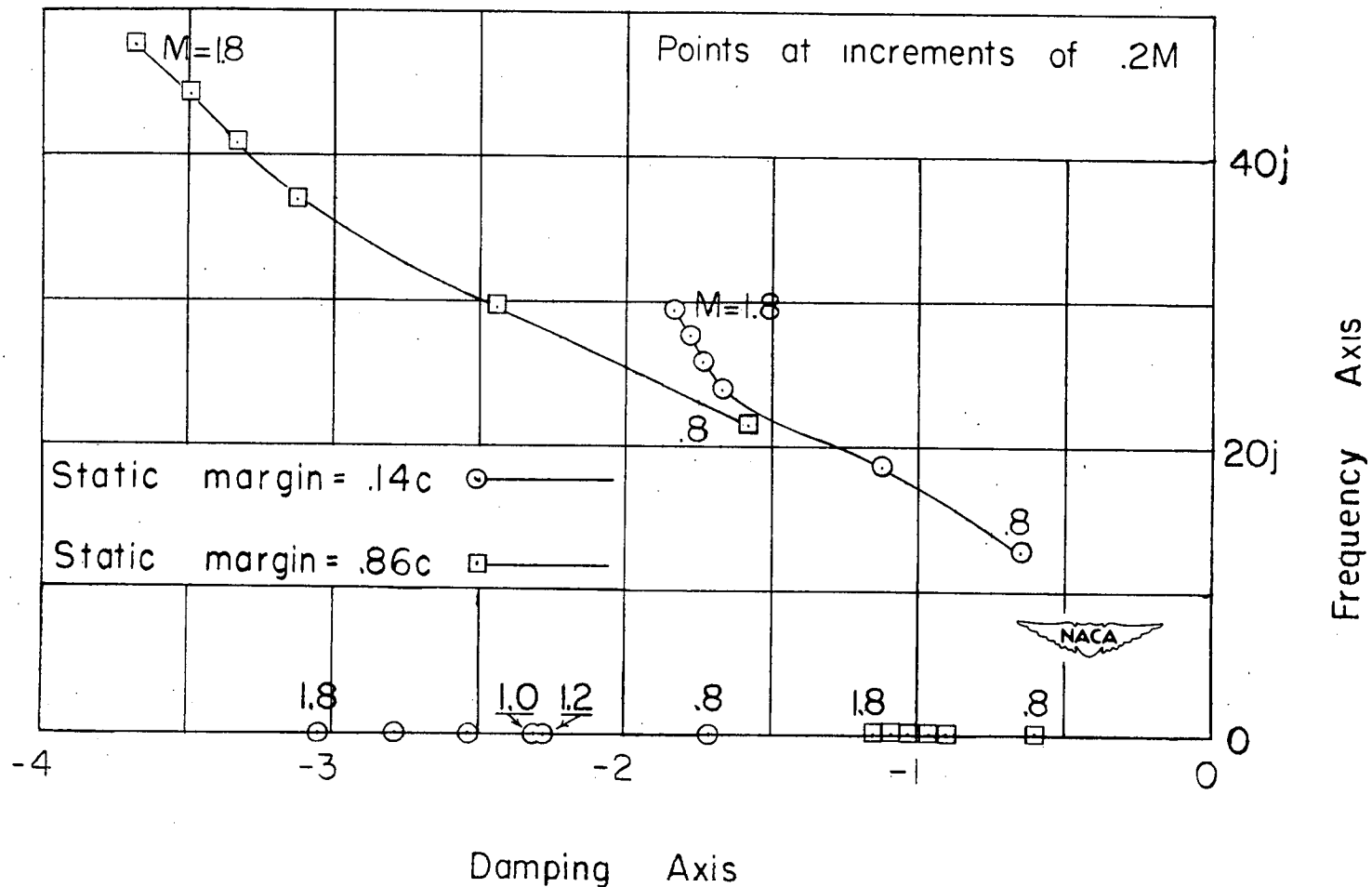
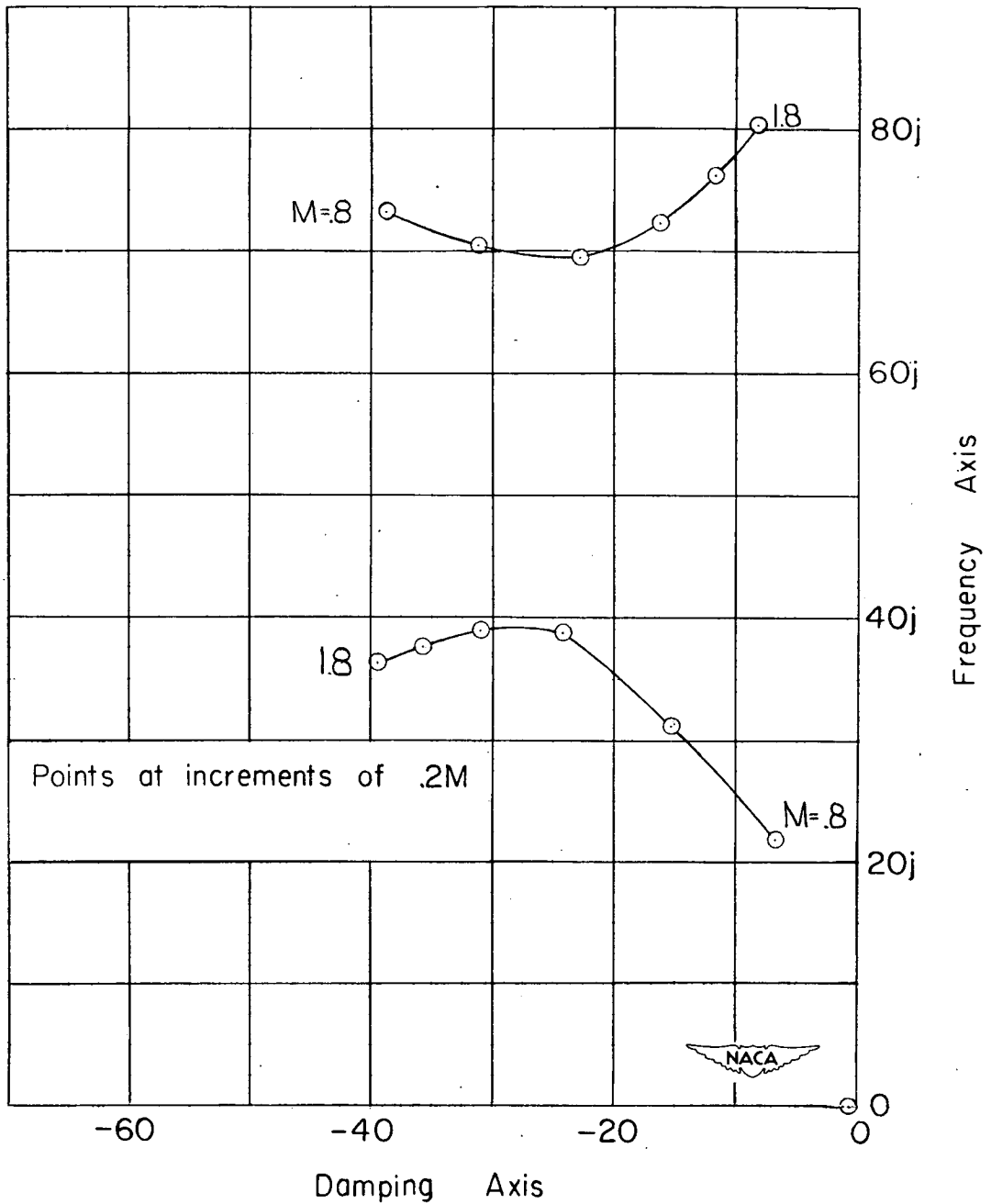
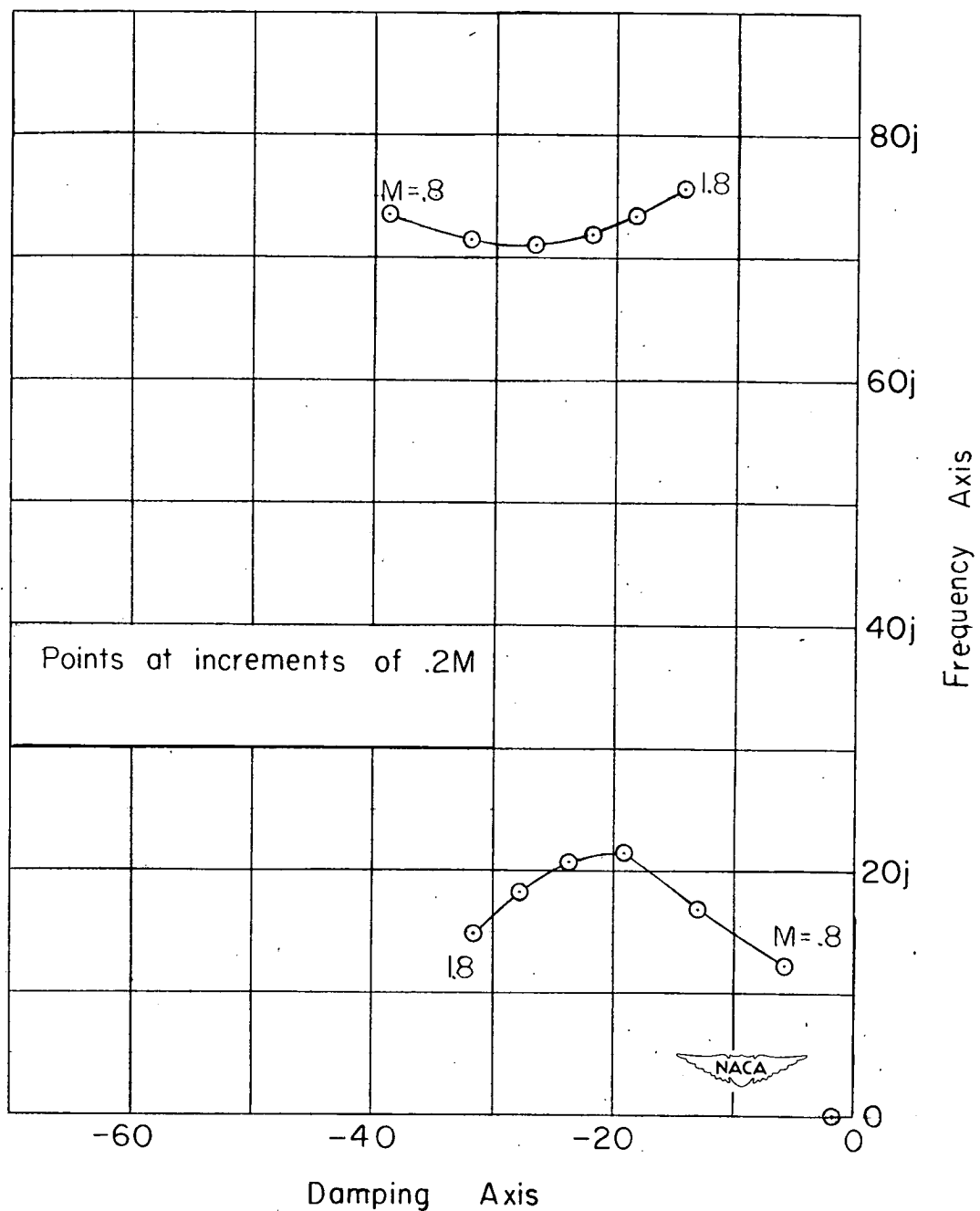


Figure 19.- Locus of roots of the closed-loop characteristic equation of  $\frac{\theta_o}{\theta_i}(p)$  representing the longitudinal response of the missile with no auxiliary damping showing Mach number effect.  $K_A = 1.0$ ; sea level.



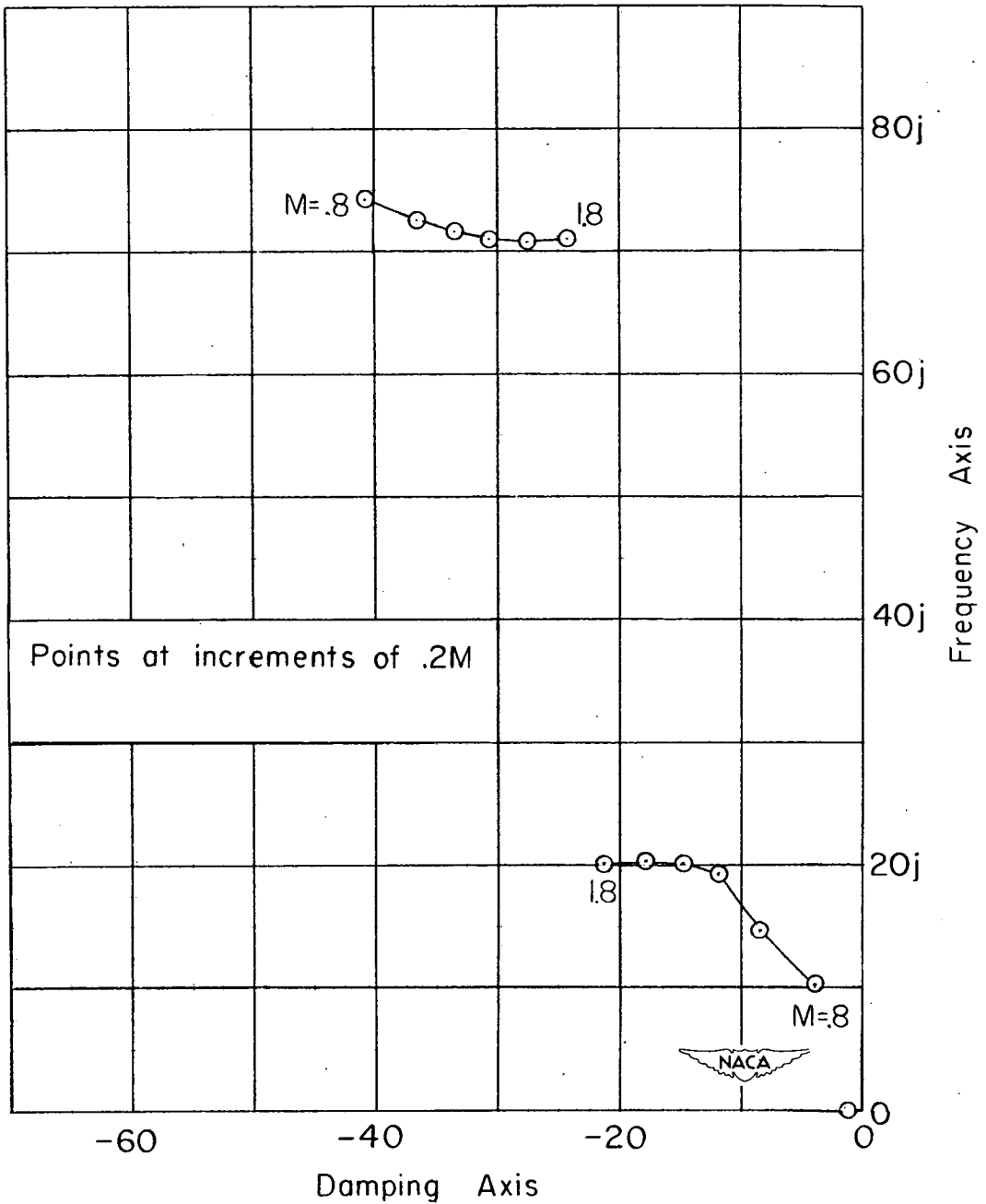
(a) Sea level; static margin = 0.86c.

Figure 20.- Locus of roots of the closed-loop characteristic equation of  $\frac{\theta_o}{\theta_i}(p)$  representing the longitudinal response of the missile with auxiliary damping. Mach number effect and the magnitude of the largest real root are shown.  $K_A = 1.0$ .



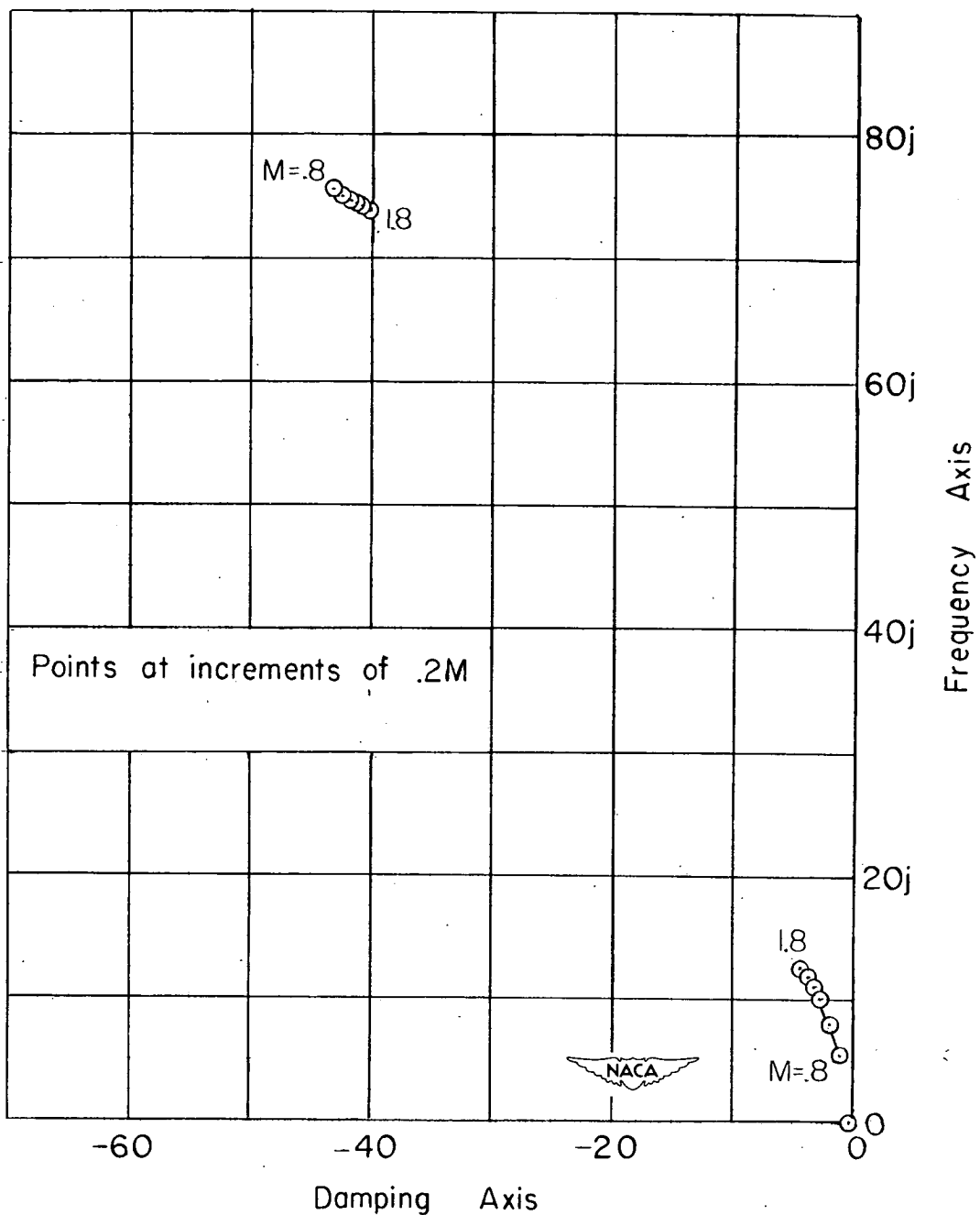
(b) Sea level; static margin = 0.14c.

Figure 20.- Continued.



(c) 10,000 feet; static margin = 0.14c.

Figure 20.- Continued.



(d) 40,000 feet; static margin = 0.14c.

Figure 20.- Concluded.